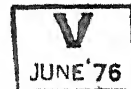


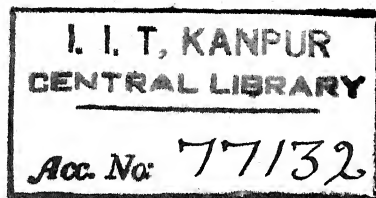
1. STABILITY BOUNDARIES OF A REACTOR BY THE
D-PARTITION METHOD
2. DIGITAL SIMULATION OF A BOILING WATER
REACTOR CORE AND SECONDARY STEAM GENERATOR

A Thesis presented to the
Faculty of Electrical Engineering
in partial fulfilment of the requirements of the
Degree of Master of Technology.



Approved.....*V. R. Saxty*.....(Thesis Advisor)

.....*M. a. Pai*.....



Thesis
621.314
Sh 13 A

M. a. Pai

Shri Kant Shah
Indian Institute of Technology
Kanpur
August 1967

EE-1967-M-~~18~~ SHA-STA

ACKNOWLEDGEMENT

The author wishes to convey his sense of deep debt to Professor V.R. Sastry for his enthusiasm, advice, suggestions and critical appraisal.

The author is also grateful to the Ministry of Education, Government of India for financing the studies under the Technical Teachers' Training Programme and to Professor H.K. Kesavan, Head, Department of Electrical Engineering for providing the necessary facilities.

ABSTRACT

✓ The first part of this thesis deals with the problem of determination of stable regions of operation of a reactor and ^{the} second with the representation of certain components of a dual cycle boiling reactor power plant for dynamic studies. ✓

✓ The maximum permissible moderator and fuel temperatures, their time constants, etc. in a nuclear reactor will depend upon the choice of the fuel element, lattice structure, etc. X Further, during the operation of a graphite power reactor the moderator temperature coefficient may vary from -2×10^{-5} to $15 \times 10^{-5} \text{ } \delta_k / ^\circ\text{C}$. Thus, ✓ at the preliminary design stage (in view of the uncertainties in some parameters) the mathematical model of a reactor can be reduced to a multiparameter linear system. The conventional methods of determination of the stability boundaries of a multiparameter linear system are either too tedious or time consuming or both. It has been illustrated in this thesis that the D-Partition method when used in conjunction with a digital computer yields the stability boundaries much more easily. ✓

✓ In the second part of the thesis mathematical models for the boiling water reactor core and the secondary steam generator for digital simulation are discussed. The mathematical model for the reactor core incorporates the delayed neutron effects and the reactivity feedback terms due to the variations in the fuel temperature and the void fraction. ✓

✓ The mathematical model for the secondary steam generator is developed with the assumption that it can be

represented adequately for dynamic studies by an equivalent counterflow heat exchanger in which change of phase occurs. In both cases the nonlinear algebraic and differential equations are linearised around the steady-state operation point using perturbation techniques. The resulting responses of the reactor and the secondary steam generator for typical step disturbances are studied using a digital computer. ✓

TABLE OF CONTENTS

	Page
SECTION 1 - STABILITY BOUNDARIES OF A REACTOR BY THE D-PARTITION METHOD.	1
1.1 INTRODUCTION	1
1.2 MATHEMATICAL MODEL OF A GRAPHITE POWER REACTOR	2
1.3 THE D-PARTITION METHOD	3
1.4 DETERMINATION OF THE STABILITY BOUNDARIES	5
1.5 CHOICE OF VALUES OF ω FOR COMPUTATION OF STABILITY BOUNDARIES	6
1.6 DISCUSSION OF THE RESULTS ..	6
SECTION 2 - DIGITAL SIMULATION OF A BOILING WATER REACTOR CORE	10
2.1 INTRODUCTION	10
2.2 MATHEMATICAL MODEL OF THE REACTOR CORE	11
2.3 REACTOR RESPONSE FOR A STEP CHANGE IN REACTIVITY	17
2.4 EFFECT OF INLET SUBCOOLING ..	18
SECTION 3 - DIGITAL SIMULATION OF A SECONDARY STEAM GENERATOR	20
3.1 SIMPLIFYING ASSUMPTIONS ..	20
3.2 EQUATIONS FOR THE ECONOMISING REGION	21
3.3 EQUATIONS FOR THE EVAPORATING REGION	22
3.4 LINEARIZED EQUATIONS OF THE SECONDARY STEAM GENERATOR	23

3.5	DETERMINATION OF THE COEFFICIENTS OF THE VARIABLES IN THE LINEARIZED EQUATIONS	24
3.6	DISCUSSION OF RESULTS	25
SECTION 4 -	BIBLIOGRAPHY	29
SECTION 5 -	APPENDICES	31
5.1	VALUES ASSUMED FOR CALCULATIONS IN SECTION 1	31
5.2	CHARACTERISTIC EQUATION OF THE MODEL IN SECTION 1.2	31
5.3	EVALUATION OF α_m , α_k , Δ AND T ..	33
5.4	AVERAGING OF TEMPERATURES IN A COUNTERFLOW HEAT EXCHANGER	35
5.5	LINEARIZATION OF THE EQUATIONS OF THE MATHEMATICAL MODEL OF SECONDARY STEAM GENERATOR	38
5.6	PROGRAMME LISTING OF HAMMING'S NUMERICAL INTEGRATION ROUTINE	47
	FIGURES	

LIST OF PRINCIPAL SYMBOLS

(A) SYMBOLS USED IN SECTION 1

- P = Ratio of deviation in neutron flux to steady-state neutron flux.
- X_{∞} = Steady-state xenon-135 concentration in infinite flux.
- X_0 = Steady-state xenon-135 concentration in steady-state flux divided by $X_{\infty} = \frac{\sigma_x \phi_0}{\lambda_x + \sigma_x \phi_0}$
- X = Deviation in xenon-135 concentration divided by X_{∞} .
- I = Deviation in iodine-135 concentration divided by X_{∞} .
- G_1 = Difference between statistically weighted mean fuel and coolant inlet temperatures at full power, steady-state, °C.
- G_2 = Difference between statistically weighted mean moderator and coolant inlet temperatures at full power, steady-state, °C.
- T_u = Deviation of mean fuel temperature, °C.
- T_m = Deviation of mean moderator temperature, °C.
- T_1 = Fuel time constant, secs.
- T_2 = Moderator time constant, secs.
- ϕ_0 = Equilibrium flux, neutrons/cm²-sec.
- α_u = Reactivity temperature coefficient of fuel, $\delta_k / ^\circ\text{C}$.
- α_k = Controller gain δ_k per sec. per °C.
- α_x = Reactivity coefficient of xenon-135.
- σ_x = Microscopic cross-section of xenon-135 for thermal neutron capture, cm².

- λ_1 = Radioactive decay constant of iodine-135, sec.⁻¹.
 λ_x = Radioactive decay constant of xenon-135, sec.⁻¹.
 k = Multiplication factor.
 k_c = Change in k due to the operation of a control rod.
 s = Laplace's operator.

(B) SYMBOLS USED IN SECTION 2

- A = Area, sq. ft.
 C_i = Concentration of i^{th} group of delayed neutrons, nuclei/cm³.
 T = Temperature, °F.
 U = Overall heat transfer coefficient, B.Th.U./sec.-°F.
 l^* = Neutron generation time, secs.
 n = Neutron density, neutrons/cm³.
 α_v = Void fraction coefficient of reactivity.
 α_f = Fuel temperature coefficient of reactivity, $\delta k/\delta T$.
 β = Total fraction of delayed neutrons.
 β_i = Fraction of delayed neutrons of i^{th} group.
 λ_i = Decay constant of i^{th} group of delayed neutrons, cm⁻¹.

SUBSCRIPTS

- c = Coolant.
 cs = Cladding to steam.
 cw = Cladding to water.
 f = Fuel.
 fc = Fuel to cladding.

SAT = Saturated vapour.

(C) SYMBOLS USED IN SECTION 3

T = Temperature, °F.

\bar{T} = Mean temperature, °F.

W = Weight flow, lbs./sec.

x = Distance from entrance of secondary heat exchanger to boiling point, ft.

M = Mass per foot length, lbs.

P = Steam pressure.

h = Heat transfer coefficient, B.Th.U./sec.-°F.

p = Perimeter (in association with h), ft.

h_1 = Latent heat, B.Th.U./lb.

SUBSCRIPTS

p = Primary side.

s = Secondary side.

w = Water.

s = Steam.

i = Inlet.

o = Outlet.

For denoting temperatures three indices notation is used. The first shows the primary or secondary side, the second denotes the phase, and the third denotes whether it is input or output quantity. Thus, T_{pwi} denotes the inlet temperature of the primary water.

1. STABILITY BOUNDARIES OF A REACTOR BY THE

D-PARTITION METHOD

1.1 INTRODUCTION:

In a nuclear power reactor two types of instabilities can occur, namely (i) fundamental instability, when the total reactor power rises or falls without any appreciable change in the shape of the power distribution within the core and (ii) spatial instability, due to the power rising in one zone and falling in another even though the total reactor power is constant. The fundamental instability can be controlled by means of a control rod anywhere in the reactor whereas the control of spatial instability requires control rods at different points [1] .

In a graphite power reactor these instabilities are caused by changes in reactivity due to (i) fuel temperature, (ii) moderator temperature and (iii) xenon variations. The fuel temperature coefficient of reactivity with natural uranium is $-2 \times 10^{-5} \delta k/^{\circ}C$, mainly due to doppler broadening of the uranium-238 resonance absorption. The moderator temperature coefficient of reactivity may increase from $-2 \times 10^{-5} \delta k/^{\circ}C$ up to $+15 \times 10^{-5} \delta k/^{\circ}C$ at high irradiations of 3000MW days per tonne, due to plutonium-239 produced in the reactor by neutron absorption in uranium-238. In addition there are time lags between change in power and changes in fuel and moderator temperatures [1] . Hence for present stability analysis a point reactor model incorporating all these effects has been chosen.

The following methods are described in the literature for the conventional stability analysis of linear systems [2 to 7]
 1) Routh-Hurwitz criterion, 2) Nyquist criterion, 3) root locus techniques and 4) analog computer solution. When there are several variables, the amount of labour involved in applying any of the above techniques is prohibitively large.

For instance, with an analog computer the stability boundaries on a two parameter plane have to be determined as follows: all the variables, except two say α_m , α_k on whose plane the stability boundaries are being plotted are given numerical values. The potentiometer corresponding to α_m is set to a particular value and the value of α_k corresponding to stability boundaries is determined by a trial and error process. This is repeated for different values of α_m . This constitutes one set of results corresponding to one case. This process is repeated for as many cases as desired. The stability boundaries for one case by analog computer takes almost half a day whereas by using a digital computer (IBM 7044) and D-Partition method same stability boundaries can be evaluated in 10 secs. (execution time).

1.2 MATHEMATICAL MODEL OF A GRAPHITE POWER REACTOR:

The equations which describe the performance of the reactor model are as follows [1] :

$$\alpha_u T_u + \alpha_m T_m + \alpha_x X + k_0 = 0.07 \text{ sP} \quad (1.1)$$

$$T_u = \frac{G_1 P}{1 + 2.1 s} \quad (1.2)$$

$$sk_0 = -\alpha_k^T u \quad (1.3)$$

$$T_m = \frac{G_2 P}{1 + T_2 s} \quad (1.4)$$

$$sI = \sigma_x \beta_0 P - \lambda_1 I \quad (1.5)$$

$$sX = \lambda_1 I - (\lambda_x + \sigma_x \beta_0) X - \sigma_x \beta_0 X_0 P \quad (1.6)$$

$$X_0 = \frac{\sigma_x \beta_0}{\lambda_x + \sigma_x \beta_0} \quad (1.7)$$

The modifications of the present model have been described in the earlier references [1 and 8]. All the above equations are linearized by considering perturbations about the steady state levels corresponding to full reactor power. In the above model, a mean neutron lifetime of 70 milli-seconds has been assumed, rather than the one milli-second life time of a prompt neutron, to take into some account of the effects of the delayed neutrons. The parameters β_0 , G_1 , G_2 , T_1 and T_2 in the mathematical model of the reactor system can vary. Hence the reactor control system designer may like to know the variation of the stability boundaries on the α_m, α_k plane and natural frequencies of oscillations in the system with the variations in the parameters β_0 , G_1 , G_2 , T_1 and T_2 . Thus the present problem reduces to the stability analysis of a multiparameter linear system.

1.3 THE D-PARTITION METHOD [9, 10] :

Brief details of this method are reviewed to facilitate the understanding of the present study. In the complex s-plane,

the presence of all the roots on the left half plane ensures stability, i.e., the imaginary axis acts as the boundary for the stable and unstable regions. In the D-Partition method the imaginary axis is mapped on a two parameter plane of interest, so that the possible stable and unstable regions can be identified on this plane.

With the help of the mathematical model of the given linear system, the characteristic equation is obtained (see Appendix 5.2). Then $s = j\omega$ is substituted in the characteristic equation and real and imaginary parts are separately equated to zero. Let the resulting equations be

$$\alpha_m S_1(\omega) + \alpha_k Q_1(\omega) + R_1(\omega) = 0 \quad (1.8)$$

$$\alpha_m S_2(\omega) + \alpha_k Q_2(\omega) + R_2(\omega) = 0 \quad (1.9)$$

where α_m and α_k are the two parameters on whose plane the stability boundaries have to be plotted. Then for each value of ω , α_m and α_k can be evaluated from the following formulae:

$$\Delta = S_1 Q_2 - S_2 Q_1$$

$$\alpha_m = \frac{-R_1 Q_2 + R_2 Q_1}{\Delta}$$

$$\alpha_k = \frac{-S_1 R_2 + S_2 R_1}{\Delta}$$

For different values of ω , α_m and α_k are plotted on a right handed system of coordinates (α_m, α_k) i.e., α_m along x-axis and α_k along y-axis. In order to shade the boundary of

the curve, move along the boundary in the direction of ω -increasing and shade it on the left edge at those points for which $\Delta > 0$ and on the right edge for those points for which $\Delta < 0$. The shaded region is labelled as stable region in Figs. 1, 3, 5, 7 and 9 of this thesis. The only strict method of verifying whether the shaded region is a stable region is to apply Routh's or any other criterion for any convenient point inside this region. The rules for shading the D-Partition in some special cases are discussed in references [9 and 10] .

1.4 DETERMINATION OF THE STABILITY BOUNDARIES:

In Appendix 5.3, the formulae for the evaluation of α_m , α_k , Δ and T (for any assumed value of ω) are furnished. A digital computer programme was written for the above purpose. The input to the digital computer consists of ϕ_0 , G_1 , G_2 , T_1 , T_2 , starting and final values of ω and interval of ω . The output from the digital computer is obtained in the following format:

ω	α_m	α_k	Δ	T (period in hours)
----------	------------	------------	----------	--------------------------

These results have been plotted in Figs. 1 to 10. Figs. 1, 3, 5, 7 and 9 show the stable and unstable regions of operation for different cases. Figs. 2, 4, 6, 8 and 10 furnish the periods of oscillations at the different boundaries. Incidentally the stability boundaries indicate whether the system is conditionally stable or not. The gain margin of the system can also be obtained from these results.

1.5 CHOICE OF VALUES OF ω FOR COMPUTATION OF THE STABILITY BOUNDARIES:

Theoretically speaking, ω can take values from $-\infty$ to $+\infty$. In actual practice only a limited region will be of interest, since most parameters vary within certain bounds. In the present case, α_m can vary in a graphite moderated power reactor from -2×10^{-5} to $15 \times 10^{-5} \delta_k/\%C$. From the first digital computer run, an initial estimate of ω was made for variation of α_m between these limits. During subsequent computer runs ω was varied around this region.

1.6 DISCUSSION OF THE RESULTS:

1.6.1 EFFECT OF VARIATION OF FUEL TIME CONSTANT T_1 :

Figs. 1 and 2 show the variation of stability boundaries and periods of oscillations respectively. When T_1 is reduced to 10 secs. from 20 secs., the controller gain at the upper stability boundary is almost doubled, whereas, the periods of oscillations are reduced to $2/3$ of their earlier values. Since the results at the lower boundary are not affected, it may be concluded that variation of fuel time constant T_1 has no effect on lower stability boundary.

1.6.2 EFFECT OF VARIATION OF MODERATOR TIME CONSTANT T_2 :

The effect of variation of moderator time constant T_2 has the opposite effect on stability boundaries compared to that of fuel time constant T_1 . The results are shown in Figs. 3 and 4.

In this case the controller gain and periods of oscillations at lower stability boundary are affected and not those at the upper stability boundary. With increasing moderator time constant, the stable region of operation is increased beyond $\alpha_m = 4.5 \times 10^{-5} \delta_K / ^\circ\text{C}$, whereas it is slightly decreased below this value. Presumably at lower values of α_m , with increasing moderator time lag, there is not sufficient compensation for the negative coefficient of reactivity due to rise in fuel temperature and xenon concentration. At higher moderator temperatures, the effect of increasing the moderator time constants to 2000 secs. is to increase periods of oscillations, compared to those when $T_2 = 500$ secs.

1.6.3 EFFECT OF VARIATION OF FUEL TEMPERATURE:

Since G_1 is the difference between fuel and coolant inlet temperatures, this effect can be studied by modifying G_1 suitably. Figs. 5 and 6 show the results for this case. With increasing G_1 , the stable region of operation is increased due to the downward shifting of the lower boundary. The periods of oscillations are reduced to 0.018 hours with $G_1 = 675$ compared to 0.030 hours with $G_1 = 275$. The controller gain at the upper stability boundary is not affected.

1.6.4 EFFECT OF VARIATION OF MODERATOR TEMPERATURE:

This case was studied by increasing G_2 to 175 from 120. From Fig. 7, it can be seen that the stable region of

operation is decreased with increase in G_2 by upward shift of the lower stability boundary. The upper stability boundary is not affected. Fig. 8 shows that the periods of oscillations near the lower boundary decrease with increasing G_2 . They are not altered near the upper boundary. Thus G_2 affects only the lower stability boundary and not the upper one.

1.6.5 EFFECT OF VARIATION OF EQUILIBRIUM FLUX LEVEL β_0 :

The effect of variation of equilibrium flux level on fundamental and spatial instabilities in a reactor have been investigated in reference [7]. Only the fundamental instability can be investigated using a point reactor model similar to the present one. The equations of the mathematical model in Section (1.2) can be obtained from the kinetic equations of the model in reference [7] by assuming that the power excursions in both regions are equal and in phase. Hence it is reasonable to expect that the stability regions and periods of oscillations agree with those obtained in reference [7], which indeed is the case. Hence these results are not plotted here.

1.6.6 EFFECT OF SIMULTANEOUS VARIATION OF G_1 AND G_2 :

As would be expected the results are a combination due to variations in G_1 and G_2 . Figs. 9 and 10 show these results. The stable region of operation is increased by downward shift of the lower boundary while the upper stability boundary is not affected. The periods of oscillations near the lower stability boundary have increased while those at the upper boundary have decreased.

1.7 CONCLUSIONS:

In the design of a plant control system, in which there are several parameters that are subject to variation, the advantages of D-Partition method for computation of stability boundaries, compared to other approaches is best illustrated by the case discussed earlier. At the same time it must be pointed out that much of the simplicity of this method is lost if the two parameters on whose plane stability boundaries are being plotted appear as nonlinear terms. Further information regarding transient response of the system cannot be obtained easily by this method, though an approach has already been made to evaluate the transient response using this method in reference [10] . For stability boundary calculations other approaches like root locus technique, analog computer solutions, etc. are rather tedious. But they are useful for the synthesis of the control system, taking into account the desired transient response. Hence it may be preferable to use in the preliminary design stage the D-Partition method. In the final design stages, when choice of most of the parameters is nearly complete, other approaches can be used for control system synthesis purposes.

2. DIGITAL SIMULATION OF A BOILING WATER

REACTOR CORE

2.1 INTRODUCTION [12, 13] :

There are several variations of the boiling water-reactor. However, they fall into two main categories, namely, (i) Direct-Cycle System and (ii) Dual-Cycle Systems. In the direct cycle system the water is boiled in the reactor pressure vessel and steam is fed directly to the turbine. The coolant may either be forced through the core by means of a circulating pump or natural convection may be used. The direct cycle reactor has the disadvantage of not following the turbine load demand. As more steam is called for, the reactor pressure is decreased, thus increasing the steam void fraction and decreasing the reactivity, although an increase is actually required. In the dual cycle system, part of the energy from the reactor forms steam directly which is fed to the turbine, but part of the hot water produced in the reactor is pumped to a (secondary) steam generator. Additional steam is formed in this generator and is used to supply the turbine, the cooled water being returned to the reactor. An increase in turbine demand thus results in a decrease in temperature of the water and, consequently, an increase in reactivity. Because of its numerous advantages, most of the boiling water reactors are being built with dual-cycle principle. The 380MW plant under construction at Tarapore is also of the dual cycle type.

A schematic of the dual-cycle power plant is shown in

Fig. 11, which gives the relative disposition of various units of the system. In this section the simulation of boiling water reactor core is discussed.

2.2 MATHEMATICAL MODEL OF THE REACTOR CORE:

The following simplifying assumptions are made to obtain a reactor core model incorporating the essential features:

1. In the axial direction of the core, sinusoidal addition of heat has been assumed. Boiling and non-boiling lengths are calculated from inlet subcooling and heat added in an average channel per lb. of water. The cross-section of the average channel is deduced on the basis of a unit cell geometry. Dimensions of the average channel are shown in Fig. 12.
- 2(a) For the purpose of heat transfer the channel is assumed to be comprising of two regions: (i) the non-boiling and, (ii) the boiling region. The heat transfer coefficients from cladding to the coolant in both the regions have been assumed to be independent of flow and their values have been calculated using steady-state heat transfer data.
- 2(b) The heat transfer along the axial direction is considered to be negligible compared to that in the radial direction.
3. The pressure drop along the length of the channel is assumed to be negligible.
4. All the neutrons are supposed to be thermal, so that

the single group theory can be applied.

5. The neutron flux is assumed to be independent of space variables.
6. The reactivity feedback effects due to change in fuel temperature and void fraction are calculated from the data relating to an average channel. It is assumed that such a simulation represents approximately the total core response.

Thus the model is limited to the study of fundamental mode oscillations only. The kinetic equations of the reactor are as follows [12] :

$$\frac{d}{dt} n = \frac{\delta_k - \beta}{l^*} n + \sum_{i=1}^{i=6} \lambda_i C_i \quad (2.1)$$

$$\frac{d}{dt} C_i = \frac{\beta_i}{l^*} n - \lambda_i C_i \quad (2.2)$$

$$\delta_k = \Delta k_0 + \alpha_f \Delta T_f + \alpha_v \Delta V \quad (2.3)$$

Equations (2.1) and (2.2) were linearized using perturbation theory around the steady state. The linearized equations in terms of perturbations from steady-state are given below:

$$\begin{aligned} \frac{d}{dt} \Delta n = & -\frac{\beta}{l^*} \Delta n + \sum_{i=1}^{i=6} \lambda_i \Delta C_i \\ & + \frac{1}{l^*} \delta_k (n_0 + \Delta n) \end{aligned} \quad (2.4)$$

[Note: The nonlinear term $\frac{\delta k \cdot \Delta n}{1^*}$ is retained in equation (2.4)] .

$$\frac{d}{dt} \Delta C_1 = \frac{\beta_1}{1^*} \Delta n - \beta_1 \Delta C_1 \quad (2.5)$$

$$\text{where } \beta = \sum_{i=1}^{i=6} \beta_i \quad (i = 1 \text{ to } 6)$$

The values for λ_1 's and β_1 's for U-235 fuel are given in Table 2.1.

TABLE 2.1
DELAYED NEUTRON CONSTANTS

Delayed Neutron Group No.	Delay Constant	Fraction of Total Neutrons
1	1	1
1	0.0124	0.00021
2	0.0305	0.00141
3	0.1110	0.00127
4	0.3010	0.00255
5	1.1000	0.00074
6	3.0000	0.00027

2.2.1 RADIAL HEAT TRANSFER FROM FUEL TO THE COOLANT [14] :

As can be seen from Fig. 12, the total channel length is divided into two regions, occupied by (i) the steam vapour, (ii) the water. Let P_1 and P_2 be the average heat generation

rates per unit length of the fuel rod in regions 1 and 2 respectively.

The equations for the region (1) can be written as follows:

In any consistent system of units, per unit length of the fuel rod and for a small duration of time dt secs.:

The heat energy utilised in raising the fuel temperature	=	Heat generated in the fuel rod due to fissions in region 1	-	Heat trans- ferred to the cladding.
---	---	---	---	---

This can be symbolically written as

$$\rho_f A_f C_f \frac{d}{dt} T_{f1} = P_1 - (T_{f1} - T_{c1}) A_{fc} U_{fc1} \quad (2.6)$$

Similarly the following equation can be written for the rate of rise of the cladding temperature in region 1:

$$\rho_c A_c C_c \frac{d}{dt} T_{c1} = (T_{f1} - T_{c1}) A_{fc} U_{fc1} - (T_{c1} - T_{SAT}) A_{cs} U_{cs} \quad (2.7)$$

For the second region, the corresponding equations are as follows:

$$\rho_f A_f C_f \frac{d}{dt} T_{f2} = P_2 - (T_{f2} - T_{c2}) A_{fc} U_{fc2} \quad (2.8)$$

and

$$\rho_c A_c C_c \frac{d}{dt} T_{c2} = (T_{f2} - T_{c2}) A_{fc} U_{fc2} - (T_{c2} - T_w) A_{cw} U_{cw} \quad (2.9)$$

T_w , the average temperature of the water in the non-

boiling region is assumed for simplicity as

$$T_w = \frac{T_{w1} + T_{SAT}}{2}$$

Now considering perturbations from the steady state the above equations yield

$$\frac{d}{dt} \Delta T_{f1} = \frac{\Delta P_1}{\rho_f A_f C_f} - (\Delta T_{f1} - \Delta T_{c1}) \frac{A_{fe} U_{fe1}}{\rho_f A_f C_f} \quad (2.10)$$

$$\frac{d}{dt} \Delta T_{c1} = (\Delta T_{f1} - \Delta T_{c1}) \frac{A_{fe} U_{fe1}}{\rho_c A_c C_c} - (\Delta T_{c1} - \Delta T_{SAT}) \frac{A_{cs} U_{cs}}{\rho_c A_c C_c} \quad (2.11)$$

$$\frac{d}{dt} \Delta T_{f2} = \frac{\Delta P_2}{\rho_f A_f C_f} - (\Delta T_{f2} - \Delta T_{c2}) \frac{A_{fe} U_{fe1}}{\rho_f A_f C_f} \quad (2.12)$$

$$\frac{d}{dt} \Delta T_{c2} = (\Delta T_{f2} - \Delta T_{c2}) \frac{A_{fe} U_{fe1}}{\rho_c A_c C_c} - (\Delta T_{c2} - \Delta T_w) \frac{A_{cw} U_{cw}}{\rho_c A_c C_c} \quad (2.13)$$

The values for various heat transfer coefficients have been calculated from the steady-state heat transfer data.

2.2.2 CALCULATION OF BOILING AND NON-BOILING HEIGHTS:

In any typical channel, there will be two regions, one occupied mainly by water and the other by wet steam. Non-boiling height (H_0 in Fig. 13) corresponds to the region in which only sensible heat is added to the incoming subcooled coolant at the channel bottom. At $z = H_0$, the coolant becomes saturated. The remainder of the channel is that in which boiling takes place and is called the boiling height H_B .

Some subcooled boiling may of course occur in H_0 but can be neglected for all practical purposes. The ratios H_0/H and H_s/H may be evaluated from the ratio of sensible heat added to total heat added in the channel.

Assuming sinusoidal heat addition in the axial direction of the channel, maximum heat addition rate per foot length of the channel will occur at the center of the channel. Referring to Fig. 13

$$q_{\max} = \frac{q_t \times \pi}{H \times 2} \quad \text{BTHU/ft. sec.}$$

Since q_s is the heat added per lb. of water in the subcooled region

$$q_s = \int_0^{H_0} q_{\max} \sin \frac{\pi z}{H} dz$$

or

$$q_s = \frac{q_{\max} H}{\pi} \left[-\cos \frac{\pi z}{H} \right]_0^{H_0}$$

Substituting for q_{\max} and simplifying

$$\frac{q_s}{q_t} = 1/2 \left[1 - \cos \left(\pi H_0/H \right) \right]$$

or

$$H_0 = \frac{H}{\pi} \cos^{-1} \left[1 - 2(q_s/q_t) \right] \quad (2.14)$$

2.2.3 CALCULATION OF AVERAGE VOID FRACTION:

Void fraction at any section is defined by the equation

$$\alpha = \frac{\text{Volume of vapour in the mixture}}{\text{Total volume of steam water mixture}}$$

In a flow system as per the development in reference [13]

$$\alpha = \frac{1}{1 + \frac{(1-x)}{x} \times \left(\frac{v_f}{v_g}\right) S} \quad (2.15)$$

where $S \triangleq$ Slip = Ratio of the velocity of the vapour to that of the fluid.

To find the average void fraction, the total boiling length of channel is divided into a number of small segments (20 in the present case). The steam quality factor is calculated at each of these sections and using the relationship in equation (2.14), void fractions at these sections are evaluated. The total area under the void fraction curve is found by applying trapezoidal rule. The average void fraction over the entire length of the channel is found by dividing the area by the height of the channel.

Equations (2.3), (2.4), (2.5) and (2.10) to (2.15) constitute the mathematical model of the reactor core.

2.3 REACTOR RESPONSE FOR A STEP CHANGE IN REACTIVITY:

The differential equations describing the reactor model are solved using Hamming's Numerical Integration method. Runge-

Kutta method has been used for starting the solution. The programme listing is given in Appendix 5.6. Reactor responses for step reactivity disturbances of magnitude 2×10^{-4} and 4×10^{-4} were studied. The results obtained for reactivity disturbance of 4×10^{-4} were similar to those obtained with a disturbance of 2×10^{-4} . Hence only the latter case has been discussed below.

Fig. 14 shows the variations with time, of perturbations in neutron density/cm³ (Δn) and average fuel temperature, °F (ΔT_f). It can be seen that immediately after step increase in reactivity, there is a rapid rise in the neutron density. The peak value occurs at about 0.2 secs. after which neutron density starts decreasing. The average fuel temperature also increases, first slowly and then rapidly until it reaches a maximum of 0.75 °F after about 0.7 secs. Later due to negative reactivity feedback from increased fuel temperature and voids, the neutron density starts decreasing. For a small time the neutron density goes slightly below the steady state level and after 2 secs. assumes an almost steady value. The new steady state is about 0.03 percent higher than the old steady-state value. Thus it can be seen that even without any external control system the boiling water reactor has got self limiting characteristics.

2.4 EFFECT OF INLET SUBCOOLING:

Fig. 15 shows the variations in neutron density and average fuel temperature with time, when there is a step change

in inlet subcooling. The case plotted here is obtained when there is a step change of + 2% of subcooling corresponding to a step change of approximately -0.04% in coolant inlet temperature. The general nature of the response is similar to the previous case. The steady state neutron density is around 0.02% higher than the full load value. With an increase in load, the primary fluid in the secondary heat exchanger loses more sensible heat. Consequently there is an increase in the core inlet subcooling with increase in load. The present results indicate that the steady state neutron density (and hence the reactor thermal output) increases with increase in inlet subcooling. Hence a dual cycle boiling water reactor plant has got the load following characteristic.

3. DIGITAL SIMULATION OF A SECONDARY STEAM GENERATOR

In a dual cycle boiling water reactor power plant, secondary steam generator is an important element. Hence its representation is discussed in this section.

3.1 SIMPLIFYING ASSUMPTIONS:

The following assumptions have been made in formulating the mathematical model of a secondary steam generator.

- (i) The secondary steam generator can be represented by an equivalent counterflow heat exchanger.
- (ii) The kinetic and potential energies of primary and secondary liquids are small and can be neglected.
- (iii) The conduction of heat in the direction of flow is negligible in both the liquids and the metal.
- (iv) The thermal conductivity of the metal in the direction perpendicular to the flow is such that the thermal resistance of the metal wall is negligible compared to the film resistances.
- (v) Perfect mixing occurs in the liquids such that the temperature of the liquid at any section perpendicular to the flow is constant.
- (vi) There is no pressure drop in the evaporating region.
- (vii) The heat transfer coefficient between water and metal is proportional to $(\text{mass flow})^{0.8}$
- (viii) The relationship between heat flux Q/A and the superheat $(T_m - T_{SAT})$ can be correlated by the expression

$$Q/A = K (T_M - T_{SAT})^{3.5}$$

A rigorous mathematical analysis of the counterflow heat exchanger results in a set of partial differential equations since the temperatures of the liquid and the metal are both space and time dependent. These are usually difficult to solve. To obtain a simpler mathematical model "point equation" approach is used, i.e., temperatures are averaged over length in each region.

Fig. 16 shows the two regions of the heat exchanger. One of these regions in which secondary water is being raised to the saturation temperature is equivalent to an economiser and the other to a heat exchanger having a constant temperature T_{SAT} on one side.

3.2 EQUATIONS FOR THE ECONOMISING REGION:

The equations for the economising region can be written as follows. In any consistent system of units during any time (say, in one sec.)

Heat lost by primary liquid per unit length in the economising region

= Heat transferred to the metal per unit length (by conservation of energy)

$$\frac{Q_W W_{PW}}{x} [T_{pwc} - T_{pwo}] = k_1 (W_{pw})^{0.8} p_p (\bar{T}_{pw2} - \bar{T}_{m2}) \quad (3.2)$$

In a unit length and during a small interval of time 'dt' sec.

Heat utilised in raising the metal temperature = Heat transferred to the metal by primary liquid - Heat transferred by the metal wall to the secondary liquid

$$C_m M_m \frac{d}{dt} \bar{T}_{m2} = k_1 (W_{pw})^{0.8} p_p (\bar{T}_{pw2} - \bar{T}_{m2}) - k_1 (W_{sw})^{0.8} p_s (\bar{T}_{m2} - \bar{T}_{sw2}) \quad (3.3)$$

Considering unit length along the heat exchanger (on the secondary water side) during a small interval of time 'dt' secs.

Heat utilised to raise the temperature of the secondary water + Heat carried away by the secondary water = Heat transferred to the secondary water by the metal

$$C_w M_{sw} \frac{d}{dt} \bar{T}_{sw2} + \frac{C_w W_{sw}}{x} (T_{SAT} - T_{sw1}) = k_1 (W_{sw})^{0.8} p_s (\bar{T}_{m2} - \bar{T}_{sw2}) \quad (3.4)$$

Based on the procedure for averaging the temperatures in a region explained in Appendix 5.4

$$\bar{T}_{pw2} = a_2 T_{pwc} + b_2 T_{pwo} \quad (3.5)$$

$$\bar{T}_{sw2} = a_2 T_{SAT} + b_2 T_{sw1} \quad (3.6)$$

3.3 EQUATIONS FOR THE EVAPORATING REGION:

By similar reasoning, the equations for the evaporating side can be written as

$$\frac{C_w W_{pw}}{(1-x)} [T_{pwi} - T_{pwc}] = k_1 (W_{pw})^{0.8} p_p (\bar{T}_{pw1} - \bar{T}_{m1}) \quad (3.7)$$

$$C_{m1} M_1 \frac{d}{dt} \bar{T}_{m1} = k_1 (W_{pw})^{0.8} p_p (\bar{T}_{pw1} - \bar{T}_{m1}) - k_2 p_s (\bar{T}_{m1} - T_{SAT})^{3.5} \quad (3.8)$$

$$\bar{T}_{pw1} = a_1 T_{pwi} + b_1 T_{pwc} \quad (3.9)$$

If T_{SAT} and T_{sw1} are slowly varying, then \bar{T}_{sw2} is also slowly varying (see equation 3.6). Under such circumstances $\frac{d}{dt} \bar{T}_{sw2}$ in equation (3.4) is negligible and consequently x is given by

$$x = \frac{C_w W_{sw} (T_{SAT} - T_{sw1})}{k_1 p_s (W_{sw})^{0.8} (\bar{T}_{m2} - \bar{T}_{sw2})} \quad (3.10)$$

Also, from assumption (viii)

$$W_{ss} = \frac{k_2 p_s (\bar{T}_{m1} - T_{SAT})^{3.5}}{h_2} (1-x) \quad (3.11)$$

3.4 LINEARISED EQUATIONS OF SECONDARY STEAM GENERATOR:

Equations (3.2) to (3.11) are the performance equations describing the secondary heat exchanger. For digital simulation, these equations were linearised as given in Appendix 5.5. The linearized equations are given below

$$\Delta T_{pw1} = A_1 \Delta T_{pwi} + A_2 \Delta T_{m1} + A_3 \Delta W_{pw} + A_4 \Delta x \quad (3.12)$$

$$\Delta T_{pwc} = A_5 \Delta T_{pw1} + A_6 \Delta T_{m1} + A_7 \Delta W_{pw} + A_8 \Delta x \quad (3.13)$$

$$\frac{d}{dt} \Delta \bar{T}_{m1} = A_9 \Delta \bar{T}_{pw1} - A_{10} \Delta \bar{T}_{m1} + A_{11} \Delta P_{sw} + A_{12} \Delta W_{pw} \quad (3.14)$$

$$\Delta W_{ss} = A_{13} \Delta \bar{T}_{m1} - A_{14} \Delta P_{sw} - A_{15} \Delta x \quad (3.15)$$

$$\Delta \bar{T}_{pw2} = A_{16} \Delta T_{pwc} + A_{17} \Delta \bar{T}_{m2} + A_{18} \Delta W_{pw} + A_{19} \Delta x \quad (3.16)$$

$$\Delta T_{pwo} = A_{20} \Delta T_{pwc} + A_{21} \Delta \bar{T}_{m2} + A_{22} \Delta W_{pw} + A_{23} \Delta x \quad (3.17)$$

$$\begin{aligned} \frac{d}{dt} \Delta \bar{T}_{m2} = & A_{24} \Delta \bar{T}_{pw2} - A_{25} \Delta \bar{T}_{m2} + A_{26} \Delta P_{sw} \\ & + A_{27} \Delta T_{sw1} - A_{28} \Delta W_{pw} - A_{29} \Delta W_{sw} \end{aligned} \quad (3.18)$$

$$\Delta x = -A_{30} \Delta \bar{T}_{m2} + A_{31} \Delta P_{sw} + A_{32} \Delta T_{sw1} + A_{33} \Delta W_{sw} \quad (3.19)$$

3.5 DETERMINATION OF THE COEFFICIENTS OF THE VARIABLES IN THE LINEARISED EQUATIONS:

From the design data of the secondary steam generator, following quantities can be obtained.

- (i) Primary water inlet temperature.
- (ii) The primary water flow rate.
- (iii) Secondary water inlet temperature.
- (iv) Secondary water flow rate.
- (v) Pressure in the evaporating region.
- (vi) Equivalent length of the counterflow heat exchanger.
- (vii) The ratio of the boiling to nonboiling lengths at full load.
- (viii) Steam quality factor for the secondary side.

(1x) The ratios of the heat transfer coefficients from the primary water to the metal (U_1) and metal to secondary water (U_2) in both the economising region and the evaporating region.

Once the steady state values are obtained, the coefficients appearing in the linearized equations can be obtained using the formulae given in Appendix 5.5.

3.6 DISCUSSION OF RESULTS:

Responses of the required variables, i.e., the secondary steam generated and the temperature of the primary water at the outlet etc. have been obtained for various step disturbances. Figs. (17) through (21) show the time variation in these quantities. To check for the validity of the results obtained, steady state values of the variables are checked for consistency as far as conservation of heat energy is concerned. Referring to Table 3.1 following observations can be made.

It is evident from the Table 3.1 that for first three disturbances, the steady state values are consistent within reasonable limits. However, the discrepancies are more pronounced for step disturbance in the secondary inlet temperature and water flow rate. Even then the results are qualitatively correct. To explain this pronounced discrepancy let us consider equation (3.4). The equation is rewritten below.

TABLE 3.1

Sl. No.	Step Change in	Amount of change	Change in T_{pwo} °F	Change in W_{ss} lbs./sec.	Change in W_{ss} calculated
1	T_{pwi}	5 °F	2.424	10.96	10.96
2	W_{pw}	350 lbs./sec.	0.259	5.454	5.23
3	P_{sw}	-10 lbs./sq.in.	-0.2686	1.205	1.15
4	T_{swi}	10 °F	-0.223	2.173	2.42
5	W_{sw}	-10 lbs./sec.	0.05	0.523	0.675

$$C_w M_{sw} \frac{d}{dt} \bar{T}_{sw2} + \frac{C_w W_{sw}}{x} (\bar{T}_{SAT} - \bar{T}_{sw1})$$

$$= k_1 (W_{sw})^{0.8} P_s (\bar{T}_{m2} - \bar{T}_{sw2})$$

From equation (3.6)

$$\bar{T}_{sw2} = a_2 \bar{T}_{SAT} + b_2 \bar{T}_{sw1}$$

In simplifying equation (3.4), it is assumed that $\frac{d}{dt} \bar{T}_{sw1}$ is when \bar{T}_{SAT} and \bar{T}_{sw1} are slowly varying. When there is a step change in \bar{T}_{sw1} , there is a step change in \bar{T}_{sw2} see equation (3.6). So the assumption $\frac{d}{dt} \bar{T}_{sw2}$ is negligible is not valid. This explains the discrepancy in results in Table 3.1 for step disturbance in \bar{T}_{sw1} . However, such step changes are not very common in practice. If this is not the case then the mathematical model can be easily modified as follows.

From equation (3.4)

$$C_w M_{sw} \frac{d}{dt} \bar{T}_{sw2} + \frac{C_w W_{sw}}{x} (\bar{T}_{SAT} - \bar{T}_{sw1})$$

$$= k_1 P_s (W_{sw})^{0.8} (\bar{T}_{m2} - \bar{T}_{sw2})$$

In the above equation the term $\frac{d}{dt} \bar{T}_{sw2}$ has to be considered. By differentiation with respect to equation (3.6) yields:

$$\frac{d}{dt} \bar{T}_{sw2} = a_2 \frac{d}{dt} \bar{T}_{SAT} + b_2 \frac{d}{dt} \bar{T}_{sw1}$$

Substituting into equation (3.4), the following equation is obtained.

$$C_w M_{sw} \left[a_2 \frac{d}{dt} T_{SAT} + b_2 \frac{d}{dt} T_{sw1} \right] + \frac{C_w W_{sw}}{x} (T_{SAT} - T_{sw1})$$

$$= k_1 p_s (W_{sw})^{0.8} (T_{m2} - T_{sw2})$$

Thus instead of calculating x from equation (3.10), x is calculated using the above equation. Since $\frac{d}{dt} T_{SAT} = \frac{d}{dp} T_{SAT} \frac{d}{dt} p$, it can be evaluated. $\frac{d T_{sw1}}{dt}$ can be evaluated if T_{sw1} variation is known from the dynamics of the other system components.

4. BIBLIOGRAPHY

1. Sastry, V.R. and Lynn, J.W., "Analogue Investigation of the Stability of Graphite Power Reactor", Proc. I.E.E., Vol.110, No.4, April 1963, p. 812.
2. Hoffman, C.H., "How to check linear system stability", Control Engineering, August 1964, p. 75.
3. Ibid, part II, Feb. '65, p.84.
4. Ibid, part III, June '65, p. 71.
5. Ibid, part IV, October '65, p.85.
6. Ibid, part V, March '66, p. 81.
7. Natesan, T.R., "Extending Routh's criterion to check the relative stability of linear systems", Journal of the Institution of Engineers (India), Vol. 47, No. 2 & 4, parts EL₂-EL₄, October and December 1966, p. 16.
8. Sastry, V.R. and Deep, G.S., "Stability boundaries variation due to delayed neutron representation in a graphite power reactor". Journal of the Institution of Engineers (India), Vol. XLVI, No.12, pt. EL 6, August 1966, p. 578.
9. Aizerman, M.A., "Theory of Automatic Control", Pergamon Press, 1963.
10. Meerov, M.V., "Introduction to the dynamics of Automatic Regulating of Electrical Machines". Butterworths, London, 1961.
11. Lenskron, R.L. and Higgins, T.J., "D-Decomposition analysis of Automatic Control Systems", Reprint No. 405 of the Engineering Experiment Station at the University of Wisconsin (U.S.A.)

12. Glasstone, S. and Sesonske, A., "Nuclear Reactor Engineering".
D. Van Nostrand Company, Inc., 1963.
13. El-Wakil, M.M., "Nuclear Power Engineering", Mc-Graw Hill
Book Company, 1962.
14. Nahavandy, Amir N., and Von Hollen, Richard F., "A Space
Dependent Dynamic Analysis of Boiling Water Reactor
Systems", Nuclear Science and Engineering, 20, 392-413
(1964).

5. APPENDICES

5.1 VALUES ASSUMED FOR CALCULATIONS IN SECTION 1.0

$$\alpha_u = -2 \times 10^{-5} \delta_K / ^\circ\text{C}$$

$$\alpha_m = -2 \times 10^{-5} \text{ to } 18 \times 10^{-5} \delta_K / ^\circ\text{C}$$

$$\alpha_x = -0.027$$

$$\lambda_1 = 2.9 \times 10^{-5} \text{ sec.}^{-1}$$

$$\lambda_x = 2.1 \times 10^{-5} \text{ sec.}^{-1}$$

$$\sigma_x = 2.3 \times 10^{-18} \text{ cm}^2$$

$$\phi_0 = 1 \times 10^{13} \text{ to } 2 \times 10^{14} \text{ neutrons/cm}^2$$

$$T_1 = 10 \text{ and } 20 \text{ secs.}$$

$$T_2 = 500 \text{ and } 2000 \text{ secs.}$$

$$\theta_1 = 275 ^\circ\text{C and } 675 ^\circ\text{C}$$

$$\theta_2 = 120 ^\circ\text{C and } 175 ^\circ\text{C}$$

5.2 CHARACTERISTIC EQUATION OF THE MODEL IN SECTION 1.2:

From equation (1.5) in section 1.2

$$I = \frac{\sigma_x \phi_0}{(s + \lambda_1)}$$

substituting the value of I in equation (1.6) and simplifying yields

$$X = \frac{G_3 (1 - T_3 s) P}{(1 + T_3 s)(1 + T_4 s)}$$

$$\text{where, } G_3 = \frac{G_X \phi_0 (\lambda_X + G_X \phi_0)}{(1-X_0)}$$

$$T_3 = \frac{1}{\lambda_1}$$

$$T_4 = \frac{1}{\lambda_X + G_X \phi_0}$$

$$T_5 = \frac{X_0}{\lambda_1 (1-X_0)}$$

From equation (1.1) substituting for α_u , T_u , T_m , α_x , X and k_0

$$\begin{aligned} & - \frac{2 \times 10^{-5} G_1 P}{(1 + T_1 s)} + \frac{G_2 \alpha_m P}{(1 + T_2 s)} - \frac{0.027 G_3 (1 - T_5 s) P}{(1 + T_3 s)(1 + T_4 s)} - \frac{G_1 \alpha_k P}{s(1 + T_1 s)} \\ & = 0.07 sP \end{aligned}$$

$$\text{Let } A_1 = -2 \times 10^{-5} G_1$$

$$A_2 = G_2$$

$$A_3 = -0.027 G_3$$

$$A_4 = -G_1$$

$$A_5 = -0.07$$

The characteristic equation on simplification yields:

$$\begin{aligned}
& A_1 [s + (T_2 + T_3 + T_4)s^2 + (T_2 T_3 + T_2 T_4 + T_3 T_4)s^3 + T_2 T_3 T_4 s^4] \\
& + A_2 \alpha_m [s + (T_1 + T_3 + T_4)s^2 + (T_1 T_3 + T_1 T_4 + T_3 T_4)s^3 + T_1 T_3 T_4 s^4] \\
& + A_3 [s + (T_1 + T_2 - T_5)s^2 + (T_1 T_2 - T_1 T_5 - T_2 T_5)s^3 - T_1 T_2 T_5 s^4] \\
& + A_4 \alpha_k [1 + (T_2 + T_3 + T_4)s + (T_2 T_3 + T_2 T_4 + T_3 T_4)s^2 + T_2 T_3 T_4 s^3] \\
& + A_5 [s^2 + (T_1 + T_2 + T_3 + T_4)s^3 + (T_1 T_2 + T_1 T_3 + T_1 T_4 + T_2 T_3 + T_2 T_4 + T_3 T_4) \\
& \quad + (T_1 T_2 T_3 + T_1 T_2 T_4 + T_1 T_3 T_4 + T_2 T_3 T_4)s^5 \\
& \quad + T_1 T_2 T_3 T_4 s^6] \\
& = 0.
\end{aligned}$$

5.3 EVALUATION OF α_m , α_k , Δ AND T_i

Substituting $s = j\omega$ in the characteristic equation derived in section 5.2 and equating real and imaginary parts separately to zero yields the following two equations.

$$\alpha_m S_1(\omega) + \alpha_k Q_1(\omega) + R_1(\omega) = 0$$

$$\alpha_m S_2(\omega) + \alpha_k Q_2(\omega) + R_2(\omega) = 0$$

where

$$S_1(\omega) = -A_2 (T_1 + T_3 + T_4) \omega^2 + A_2 T_1 T_3 T_4 \omega^4$$

$$Q_1(\omega) = A_4 - A_4 (T_2 T_3 + T_2 T_4 + T_3 T_4) \omega^2$$

$$R_1(\omega) = -B_6 \omega^6 + B_4 \omega^4 - B_2 \omega^2$$

$$S_2(\omega) = A_2 \omega - A_2 (T_1 T_3 + T_1 T_4 + T_3 T_4) \omega^3$$

$$Q_2(\omega) = A_4 (T_2 + T_3 + T_4) \omega - A_4 T_2 T_3 T_4 \omega^3$$

$$R_2(\omega) = B_5 \omega^5 - B_3 \omega^3 + B_1 \omega$$

(B_1 to B_6 are as defined below)

$$B_1 = A_1 + A_3$$

$$B_2 = A_5 + A_3 (T_1 + T_2 - T_5) + A_1 (T_2 + T_3 + T_4)$$

$$B_3 = A_5 (T_1 + T_2 + T_3 + T_4) + A_3 (T_1 T_2 - T_1 T_5 - T_2 T_5) \\ + A_1 (T_2 T_3 + T_2 T_4 + T_3 T_4)$$

$$B_4 = A_5 (T_1 T_2 + T_1 T_3 + T_1 T_4 + T_2 T_3 + T_2 T_4 + T_3 T_4)$$

$$-A_3 T_1 T_2 T_5 + A_1 T_2 T_3 T_4$$

$$B_5 = A_5 (T_1 T_2 T_3 + T_1 T_2 T_4 + T_1 T_3 T_4 + T_2 T_3 T_4)$$

$$B_6 = A_5 T_1 T_2 T_3 T_4$$

For a given value of ω ; S_1 , Q_1 , R_1 , S_2 , Q_2 and R_2 can be evaluated from the above formulae. Then Δ , α_m , α_k and T can be evaluated as follows.

$$\Delta = S_1 Q_2 - S_2 Q_1$$

$$\Delta_m = \frac{-R_1 Q_2 + R_2 Q_1}{\Delta}$$

$$\Delta_k = \frac{-S_1 R_2 + S_2 R_1}{\Delta}$$

$$\text{Period } T = \frac{2}{\pi} \times \frac{1}{3600} \text{ hours.}$$

5.4 AVERAGING OF TEMPERATURES IN A COUNTERFLOW HEAT EXCHANGER:

For a typical counterflow heat exchanger, when there is no change of phase, following differential equations describe the heat transfer.

$$C_w W_{pw} \frac{d}{dx} T_{pw} = -U_1 (T_{pw} - T_m) = -Q \quad (5.4.1)$$

$$C_w W_{sw} \frac{d}{dx} T_{sw} = -U_2 (T_m - T_{sw}) = -Q \quad (5.4.2)$$

From the above two equations,

$$T_m = \frac{U_1 T_{pw} + U_2 T_{sw}}{U_1 + U_2} \quad (5.4.3)$$

and

$$C_w W_{pw} \frac{d}{dx} T_{pw} - C_w W_{sw} \frac{d}{dx} T_{sw} = 0 \quad (5.4.4)$$

Integrating the above two equations with respect to x and using the usual boundary conditions,

$$\begin{aligned} C_w W_{pw} T_{pw} - C_w W_{sw} T_{sw} &= A \\ &= C_w W_{pw} T_{pwi} - C_w W_{sw} T_{swo} \\ &= C_w W_{pw} T_{pwo} - C_w W_{sw} T_{swi} \end{aligned} \quad (5.4.5)$$

From (5.4.5)

$$C_w W_{pw} (T_{pwi} - T_{pwo}) = C_w W_{sw} (T_{swo} - T_{swi}) \quad (5.4.6)$$

Addition of equations (5.4.1) and (5.4.2) gives

$$\frac{C_w W_{pw}}{U_1} \frac{d}{dx} T_{pw} + \frac{C_w W_{sw}}{U_2} \frac{d}{dx} T_{sw} = T_{sw} - T_{pw} \quad (5.4.7)$$

From equation (5.4.5) we have

$$C_w W_{sw} T_{sw} = C_w W_{pw} T_{pw} - A$$

or

$$T_{sw} = \frac{W_{pw}}{W_{sw}} T_{pw} - \frac{A}{C_w W_{sw}}$$

or

$$T_{sw} - T_{pw} = T_{pw} \left[\frac{W_{pw}}{W_{sw}} - 1 \right] - \frac{A}{C_w W_{sw}} \quad (5.4.8)$$

Now using (5.4.7) and substituting for $\frac{d}{dx} T_{sw}$ from (5.4.4) we have

$$C_w W_{pw} \left[\frac{1}{U_1} + \frac{1}{U_2} \right] \frac{d}{dx} T_{pw} = T_{pw} \left[\frac{W_{pw}}{W_{sw}} - 1 \right] - \frac{A}{C_w W_{sw}} \quad (5.4.9)$$

Now define

$$\left[\frac{1}{U_1} + \frac{1}{U_2} \right] = \frac{1}{U} \quad (5.4.10)$$

$$\text{and } N = \frac{1}{C_w W_{pw}} - \frac{1}{C_w W_{sw}} \quad (5.4.11)$$

Substituting in (5.4.9), we finally have

$$\frac{d}{dx} T_{pw} = -UM T_{pw} - \frac{AU}{C_w^2 W_{pw} W_{sw}} \quad (5.4.12)$$

Now integrating equation (5.4.12) with respect to x

$$T_{pw} = B e^{-UMx} - K \quad (5.4.13)$$

and

$$B = T_{pw1} + K \quad (5.4.14)$$

since $T_{pw} = T_{pw1}$ at $x = 0$.

$$\text{Where } K = \frac{A}{M C_w^2 W_{pw} W_{sw}} \quad (5.4.15)$$

$$\text{Thus, } T_{pw} = (T_{pw1} + K) e^{-UMx} - K \quad (5.4.16)$$

Similarly,

$$T_{sw} = (T_{sw0} + K) e^{-UMx} - K \quad (5.4.17)$$

From the definition $\bar{T} = \frac{1}{L} \int_0^L T dx$, following two equations result,

$$\left. \begin{aligned} \bar{T}_{pw} &= \frac{T_{pw1} + K}{UML} (1 - e^{-UML}) - K \\ \bar{T}_{sw} &= \frac{T_{sw0} + K}{UML} (1 - e^{-UML}) - K \end{aligned} \right\} \quad (5.4.18)$$

Now putting $x = L$ in equations (5.4.16) and (5.4.17) and subtracting gives

$$e^{-UML} = \frac{T_{pwo} - T_{swi}}{T_{pwi} - T_{swo}} \quad (5.4.19)$$

Thus finally we will be having

$$\begin{aligned} \bar{T}_{pw} = T_{pwi} \left(\frac{1}{UML} - \frac{e^{-UML}}{1 - e^{-UML}} \right) \\ + T_{pwo} \left(-\frac{1}{UML} + \frac{1}{1 - e^{-UML}} \right) \end{aligned} \quad (5.4.20)$$

$$= a T_{pwi} + b T_{pwo} \quad (5.4.21)$$

Similarly,

$$\bar{T}_{sw} = a T_{swi} + b T_{swo} \quad (5.4.22)$$

5.5 LINEARIZATION OF THE EQUATIONS OF THE MATHEMATICAL MODEL OF SECONDARY STREAM GENERATOR:

The performance equations of the secondary heat exchanger are linearized using small perturbation theory around an operating point.

Derivation of equation (3.12)

From equation (3.7) we have

$$\frac{Q_w W}{(L-x)} (T_{pwi} - T_{pwc}) = k_1 p_p (W_{pw})^{0.8} (\bar{T}_{pw1} - \bar{T}_{m1})$$

$$\text{or } \bar{T}_{pw1} - \bar{T}_{m1} = \frac{Q_w (W_{pw})^{0.2}}{k_1 p_p (L-x)} (T_{pwi} - T_{pwc})$$

Writing $C_w/k_p p_p = K_1$

$$(\bar{T}_{pw1} - \bar{T}_{m1}) = K_1 \frac{(w_{pw})^{0.8}}{(L-x)} (T_{pw1} - T_{pwe})$$

Since from equation (3.9) we have

$$\bar{T}_{pw1} = a_1 T_{pw1} + b_1 T_{pwe}$$

$$T_{pwe} = \frac{\bar{T}_{pw1} - a_1 T_{pw1}}{b_1}$$

Substituting,

$$(\bar{T}_{pw1} - \bar{T}_{m1}) = \frac{K_1 (w_{pw})^{0.2}}{(L-x)} \left[T_{pw1} - \left\{ \frac{\bar{T}_{pw1} - a_1 T_{pw1}}{b_1} \right\} \right]$$

Or,

$$\bar{T}_{pw1} \left(1 + \frac{K_1}{b_1} \frac{(w_{pw})^{0.2}}{(L-x)} \right) = K_1 \frac{(a_1 + b_1)}{b_1} \frac{(w_{pw})^{0.2}}{(L-x)} T_{pw1} + \bar{T}_{m1}$$

Write $K_2 = \frac{K_1 (a_1 + b_1)}{b_1} = \frac{K_1}{b_1}$ (since $a_1 + b_1 = 1$)

Or,

$$\bar{T}_{pw1} = \frac{K_2 (w_{pw})^{0.2} T_{pw1} + (L-x) \bar{T}_{m1}}{(L-x) + K_2 (w_{pw})^{0.2}}$$

Writing,

$$\text{Numerator} = N_1 = K_2 (w_{pw})^{0.2} T_{pw1} + (L-x) \bar{T}_{m1}$$

$$\begin{aligned} \therefore \Delta N_1 &= K_2 (w_{pw})^{0.2} \Delta T_{pw1} + 0.2 K_2 (w_{pw})^{-0.8} T_{pw1} \Delta w_{pw} \\ &\quad + (L-x) \Delta \bar{T}_{m1} - \bar{T}_{m1} \Delta x \end{aligned}$$

Writing $C_1 = K_2 (W_{pw})^{0.2}$

$$C_2 = 0.2 K_2 (W_{pw})^{-0.8} T_{pw1}$$

$$C_3 = L - x$$

$$C_4 = \bar{T}_{m1}$$

$$\Delta H_1 = C_1 \Delta T_{pw1} + C_2 \Delta W_{pw} + C_3 \Delta \bar{T}_{m1} - C_4 \Delta x$$

The denominator is given by

$$D_1 = K_2 (W_{pw})^{0.2} + (L-x)$$

$$\therefore \Delta D_1 = 0.2 K_2 (W_{pw})^{-0.8} \Delta W_{pw} - \Delta x$$

Writing $C_5 = 0.2 K_2 (W_{pw})^{-0.8}$

We have

$$\Delta \bar{T}_{pw1} = \frac{D_1 \Delta H_1 - H_1 \Delta D_1}{D_1^2}$$

Substituting the values for H_1 , D_1 , ΔH_1 and ΔD_1 , we obtain

$$\Delta \bar{T}_{pw1} = A_1 \Delta T_{pw1} + A_2 \Delta \bar{T}_{m1} + A_3 \Delta W_{pw} + A_4 \Delta x$$

where $A_1 = C_1 / D_1$

$$A_2 = C_3 / D_1$$

$$A_3 = (C_2 D_1 - C_5 H_1) / D_1^2$$

$$A_4 = (N_1 - C_4 D_1) / D_1^2$$

Derivation of equation (3.13)

From equation (3.9)

$$T_{pwc} = \frac{\bar{T}_{pwl} - a_1 T_{pwl}}{b_1}$$

$$\therefore \Delta T_{pwc} = \frac{1}{b_1} \Delta \bar{T}_{pwl} - \frac{a_1}{b_1} \Delta T_{pwl}$$

Substituting the value of $\Delta \bar{T}_{pwl}$ and simplifying

$$\Delta T_{pwc} = A_5 \Delta T_{pwl} + A_6 \Delta T_{m1} + A_7 \Delta W_{pw} + A_8 \Delta x$$

where $A_5 = \frac{A_1 - a_1}{b_1}$ $A_6 = \frac{A_2}{b_1}$

$A_7 = \frac{A_3}{b_1}$ $A_8 = \frac{A_4}{b_1}$

Derivation of equation (3.14)

From equation (3.8)

$$C_m M_m \frac{d\bar{T}_{m1}}{dt} = K_1 P_s (W_{pw})^{0.8} (\bar{T}_{pwl} - \bar{T}_{m1}) - K_2 P_s (\bar{T}_{m1} - T_{SAT})^{3.5}$$

Write $K_1 P_s / C_m M_m = K_3$

$K_2 P_s / C_m M_m = K_4$

or $\frac{d}{dt} \bar{T}_{m1} = K_3 (W_{pw})^{0.8} (\bar{T}_{pwl} - \bar{T}_{m1}) - K_4 (\bar{T}_{m1} - T_{SAT})^{3.5}$

Linearizing the above expression and expressing $T_{SAT} = n P_{sw}$

where m is the slope of the pressure vs. saturation temperature characteristic.

$$\frac{d}{dt} \Delta \bar{T}_{m1} = A_9 \Delta \bar{T}_{pw1} - A_{10} \Delta \bar{T}_{m1} + A_{11} \Delta P_{sw} + A_{12} \Delta W_{pw}$$

where $A_9 = K_3 (W_{pw})^{0.8}$

$$A_{10} = K_3 (W_{pw})^{0.8} + 3.5 K_4 (\bar{T}_{m1} - T_{SAT})^{2.5}$$

$$A_{11} = 3.5 K_4 (\bar{T}_{m1} - T_{SAT})^{2.5} m$$

$$A_{12} = 0.8 K_3 (W_{pw})^{-0.2} (\bar{T}_{pw1} - \bar{T}_{m1})$$

Derivation of equation (3.15)

From equation (3.11)

$$W_{ss} = \frac{k_2 p_s (L-x)}{h_1} (\bar{T}_{m1} - T_{SAT})^{3.5}$$

Writing $k_2 p_s / h_1 = K_5$

We have $\Delta W_{ss} = A_{13} \Delta \bar{T}_{m1} - A_{14} \Delta P_{sw} - A_{15} \Delta x$

Where $A_{13} = 3.5 K_5 (L-x) (\bar{T}_{m1} - T_{SAT})^{2.5}$

$$A_{14} = 3.5 K_5 (L-x) (\bar{T}_{m1} - T_{SAT})^{2.5} m$$

and $A_{15} = K_5 (\bar{T}_{m1} - T_{SAT})^{3.5}$

Derivation of equation (3.16)

From equation (3.2)

$$\frac{C_{pw} \cdot W_{pw}}{x} (T_{pwc} - T_{pwo}) = k_1 p_p (W_{pw})^{0.8} (\bar{T}_{pw2} - \bar{T}_{m2})$$

and from equation (3.5)

$$T_{pwo} = \frac{\bar{T}_{pw2} - a_2 T_{pwc}}{b_2}$$

substituting and linearizing

$$\Delta \bar{T}_{pw2} = A_{16} \Delta T_{pwc} + A_{17} \Delta \bar{T}_{m2} + A_{18} \Delta W_{pw} + A_{19} \Delta x$$

Where the coefficients are determined using following

$$K_6 = C_{pw2} / k_1 p_p$$

$$K_7 = K_6 / b_2$$

$$C_6 = K_7 (W_{pw})^{0.2}$$

$$C_7 = 0.2 K_7 (W_{pw})^{-0.8} T_{pwc}$$

$$C_8 = x$$

$$C_9 = \bar{T}_{m2}$$

$$C_{10} = 0.2 K_7 (W_{pw})^{-0.8}$$

and

$$H_2 = K_7 (W_{pw})^{0.2} T_{pwc} + x \bar{T}_{m2}$$

$$D_2 = K_7 (W_{pw})^{0.2} + x$$

Thus,

$$A_{16} = C_6 / D_2$$

$$A_{17} = C_8 / D_2$$

$$A_{18} = (C_7 D_2 - C_{10} W_2) / D_2^2$$

$$A_{19} = (C_9 D_2 - W_2) / D_2^2$$

Derivation of equation (3.17)

From equation (3.5)

$$T_{pwo} = \frac{\bar{T}_{pw2} - a_2 T_{pwo}}{b_2}$$

$$\therefore \Delta T_{pwo} = A_{20} \Delta T_{pwo} + A_{21} \Delta T_{w2} + A_{22} \Delta W_{pw} + A_{23} \Delta x$$

where, $A_{20} = (A_{16} - a_2) / b_2$

$$A_{21} = A_{17} / b_2$$

$$A_{22} = A_{18} / b_2$$

$$A_{23} = A_{19} / b_2$$

Derivation of equation (3.18)

From equation (3.6)

$$\bar{T}_{sw2} = a_2 T_{SAT} + b_2 T_{sw1}$$

or

$$\Delta \bar{T}_{sw2} = a_2 m \Delta P_{sw} + b_2 \Delta T_{sw1}$$

From equation (3.3)

$$\begin{aligned} C_m M \frac{d}{dt} \bar{T}_{m2} = & k_1 p_p (W_{pw})^{0.8} (\bar{T}_{pw2} - \bar{T}_{m2}) \\ & - k_1 p_s (W_{sw})^{0.8} (\bar{T}_{m2} - \bar{T}_{sw2}) \end{aligned}$$

Linearization of the above equation yields

$$\begin{aligned} \frac{d}{dt} \Delta \bar{T}_{m2} = & A_{24} \Delta \bar{T}_{pw2} - A_{25} \Delta \bar{T}_{m2} + A_{26} \Delta P_{sw} \\ & + A_{27} \Delta T_{sw1} - A_{28} \Delta W_{pw} - A_{29} \Delta W_{sw} \end{aligned}$$

Where, $K_8 = k_1 p_p / C_m M$

$K_9 = k_1 p_s / C_m M$

$A_{24} = K_8 (W_{pw})^{0.8}$

$A_{25} = K_8 (W_{pw})^{0.8} + K_9 (W_{sw})^{0.8}$

$A_{26} = K_9 (W_{sw})^{0.8} a_2 m$

$A_{27} = K_9 (W_{sw})^{0.8} b_2$

$A_{28} = 0.8 K_8 (W_{pw})^{-0.2} (\bar{T}_{pw2} - \bar{T}_{m2})$

$A_{29} = 0.8 K_9 (W_{sw})^{-0.2} (\bar{T}_{m2} - \bar{T}_{sw2})$

Derivation of equation (3.19)

From equation (3.10)

$$x = \frac{C_w W_{sw} (T_{SAT} - T_{sw1})}{k_1 p_s (W_{sw})^{0.8} (\bar{T}_{m2} - \bar{T}_{sw2})}$$

Linearizing the above equation yields

$$\Delta x = -A_{30} \Delta \bar{T}_{m2} + A_{31} \Delta P_{sw} + A_{32} \Delta T_{sw1} + A_{33} \Delta W_{sw}$$

where $K_{10} = C_w / k_1 p_s$

$$N_3 = K_{10} (W_{sw})^{0.2} (T_{SAT} - T_{sw1})$$

$$D_3 = (\bar{T}_{m2} - \bar{T}_{sw2})$$

$$C_{11} = K_{10} (W_{sw})^{0.2} m$$

$$C_{12} = K_{10} (W_{sw})^{0.2}$$

$$C_{13} = 0.2 K_{10} (W_{sw})^{-0.8} (T_{SAT} - T_{sw1})$$

$$A_{30} = N_3 / D_3^2$$

$$A_{31} = (D_3 C_{11} + a_1 m N_3) / D_3^2$$

$$A_{32} = (N_3 b_1 - D_3 C_{12}) / D_3^2$$

$$A_{33} = C_{13} / D_3$$

5.6 PROGRAMME LISTING OF THE HAMMING'S NUMERICAL INTEGRATION

ROUTINE:

The complete listing of the programme utilized for solving the simultaneous differential equations derived in Section 2 is given below. The same programme with suitable changes is used for solving the simultaneous differential equations derived in Section 3.

C FORTRAN IV NECESSARY

C HAMMINGS NUMERICAL INTEGRATION SCHEME FOR 1ST ORDER EQNS

C DIMENSION DERINT(25),EM(25),EMDASH(25),Y(100),YDASH(75),P(25)
1 C(25),PLESC(25),WTS(25),AR(4),BR(4),CR(4),QR(25)

C COMMON N,H,T,TO,YDASH,Y,AR,BR,CR,QR

C COMMON ISTRT

C ABSF(X)=ABS(X)

C AR(1)=0.5

AR(2)=0.29289322

AR(3)=0.17071068E+01

AR(4)=0.16666667

C BR(1)=2.0

BR(2)=1.0

BR(3)=1.0

BR(4)=2.0

C CR(1)=0.5

CR(2)=0.29289322

CR(3)=1.7071068

CR(4)=0.5

C C21B=0.92561983

C21E=0.74380163E-01

C CONTINUE

C ISTRT = 1

C READ 10,N

READ 30,T,H,FINALT,HEXIT

READ 30,(Y(I),I=1,N)

102 READ 30,A,A1,A2,A3

15 READ 30,HLEAST

READ 30,(WTS(I),I=1,N)

```

PRINT10,N
PRINT30,T,H,FINALT,HEXIT
PRINT30,(Y(I),I=1,N)
PRINT30,A,A1,A2,A3
PRINT30,HLEAST
PRINT30,(WTS(I),I=1,N)

```

C

```

T0=T

```

2

```

CONTINUE

```

```

16 CALL DERIVE(Y,DERINT)

```

```

201 CALL START (PLESC)

```

```

C251I=0.375*H

```

```

SIGMA=0.0

```

```

SUM=0.0

```

```

DO 202 I=1,N

```

```

WTSI=WTS(I)

```

```

SIGMA=SIGMA+ABSF(Y(I+75))*WTSI

```

```

ERROR= YDASH(I) + YDASH(I+25)

```

```

202 SUM=SUM+WTSI*ABSF(Y(I+ 75)-Y(I)-C251I*(ERROR+ERROR+ERROR
1 + YDASH(I+ 50)+DERINT(I)))

```

```

SUM=SUM*8.962963

```

```

IF(SIGMA-1.0)206,206,207

```

```

207 SUM=SUM/SIGMA

```

```

206 IF(SUM-A)5,5,204

```

```

204 T=T-H-H-H

```

```

H=0.5*H

```

```

IF(H-HLEAST)12,201,201

```

```

12 PRINT 80

```

```

602 PRINT 30,T

```

```

PRINT 30,(Y(I),I=1,N)

```

```

GO TO 1

```

```

5 T=T-H-H-H

```

```

2220 PRINT 320,H

```

```

222 DO 6 I = 1,51,25

```

C *****

C NEXT STATEMENT(S) DEPEND(S) UPON THE COMPILER

C *****

```

CALL OUT(HEXIT,Y(I))

```

```

6 T=T+H

```

C *****

C NEXT STATEMENT(S) DEPEND(S) UPON THE COMPILER

C *****

```

CALL OUT(HEXIT,Y(76))

```

```

101 C21A = 1.3333333*H

```

```

C21D = H+H+H

```

```

103 DO 104 I=1,N

```

```

SUM=YDASH(I)+YDASH(I+ 50)

```

```

P(I) = Y(I)+ C21A*(SUM+SUM-YDASH(I+25))

```

```

104 EM(I)=P(I)-C21B*PLESC(I)

```

```

T=T+H

```

```

CALL DERIVE(EM,ENDASH)

```

```

ERROR=0.0

```



```

SUM=0.0
DO 105 I=1,N
SIGMA= YDASH(I+ 50)
C(I)= .125*(9.*Y(I+ 75)-Y(I+25)+C21D*(EMDASH(I)+SIGMA+SIGMA-
1 (I+25)))
WTSI=WTS(I)
ERROR=ERROR+ABSF(P(I)-C(I))*WTSI
105 SUM=SUM+WTSI*ABSF(C(I))
IF(SUM-1.0)106,106,107
107 ERROR=ERROR/SUM
106 IF(ERROR-A2)108,108,109
108 DO 111 I=1,N
K1=I+25
K2=I+50
K3=I+75
Y(I)=Y(K1)
Y(K1)=Y(K2)
Y(K2)=Y(K3)
YDASH(I)=YDASH(K1)
YDASH(K1)=YDASH(K2)
PI=P(I)
CI=C(I)
PLESC(I)=PI-CI
111 Y(K3)=C21B*CI+C21E*PI
C *****
C NEXT TWO STATEMENTS DEPEND UPON THE COMPILER
C *****
CALL DERIVE(Y(76),YDASH(51))
CALL OUT(HEXIT,Y(76))
IF(FINALT-T)99,99,188
188 IF(ERROR-A1)112,112,103
112 H=H+H
125 DO 113 I=1,N
113 Y(I)=Y(I+75)
CALL START(PLESC)
GO TO 5
109 IF(ERROR-A3)123,124,124
123 T=T-H
H=0.5*H
IF (H - HLEAST)12,125,125
124 PRINT 160
GO TO 1
99 CONTINUE
GO TO 1
10 FORMAT(2I6)
30 FORMAT(8E10.3)
40 FORMAT(10X)
80 FORMAT(9HH TOO LOW)
160 FORMAT(14H ERROR OVER A3)
320 FORMAT(/20X,4H H =,E12.5//)
END

```

```

SIBFTC SUB1      NODECK,NOPRNT
SUBROUTINE START(PLESC)
DIMENSION Y(100),YDASH(75),PLESC(25),A(4),B(4),C(4),Q(25),CAY(25)
COMMON N,H,T,TO,YDASH,Y,A,B,C,Q
HALF=0.5*H
DO 22 I=1,N
22  Q(I)=0.0
DO 1 I=25,75,25
    I1=I-24
    I2=I1+N-1
DO 13 I1=I1,I2
13  Y(I1+25)=Y(I1)
DO 8 J=1,4
    AY=A(J)
    BEE=B(J)
    SEA=C(J)
*****
THE FOLLOWING STATEMENT DEPENDS UPON THE COMPILER
*****
CALL DERIVE(Y(I+1),CAY)
IF((J-1)+(I-75)*(I-50))14,15,14
15  DO 16 IJ=1,N
    JJ=IJ+I-50
16  YDASH(JJ)=CAY(IJ)
14  CONTINUE
    IF(J-J/2*2)5,3,5
5    T=T+HALF
3    CONTINUE
DO 8 II=1,N
    QTY=AY*(CAY(II)-BEE*Q(II))
    III=I+II
    Y(III)=Y(III)+QTY*H
8    Q(II)=Q(II)+3.0*QTY-SEA*CAY(II)
1    CONTINUE
*****
THE FOLLOWING STATEMENT DEPENDS UPON THE COMPILER
*****
CALL DERIVE(Y(76),YDASH(51))
DO 2 I=1,N
2    PLESC(I)=0.0
RETURN
END

SIBFTC SUB2      NODECK,NOPRNT
SUBROUTINE OUT(HEXIT,Y)
DIMENSION Y(100)
COMMON N,H,T,TO
DIMENSION SPACE(212)
COMMON SPACE,ISTRT
COMMON ALNTH,HIGHT,HZERO,FLOW,PAI,QS,CONST,TSAT,TSW,TC1,TC2,A2,A4
1    FAC1,FAC2,VOID,TFAVG
CALL CHANGE
IF(T-TO-HEXIT) 1,2,2

```

```

4   TQ=TO+HEXIT
   PRINT 20,T,Y(1),TFAVG,VOID,HZERO,Y(8),Y(10),Y(9),Y(11)
1   RETURN
20  FORMAT(6X,F10.6,4E16.4,4E10.3/)
   END
SIBFTC SUB3      NODECK,NOPRNT
      SUBROUTINE DERIVE(Y,YDASH)
C
C   DIMENSION SPACE(213)
C
C   DIMENSION Y(100), YDASH(75)
COMMON N , H , T , SPACE , ISTRT
C
COMMON ALNTH , HIGHT,HZERO,FLOW,PAI,QS,CONST,TSAT,TSW,TC1,TC2,A2,
1   A4,FAC1,FAC2,VOID
COMMON TFAVG
C
ATANF(X)=ATAN(X)
C
1   FORMAT(/8X,8H TIME      ,16H NEUTRON DENSITY,16H  AVG FUEL TEMP ,
1 5X,6H  VOID,10X,6H HZERO,8X,5H  TF1,5X,5H  TF2,5X,5H  TC1,5X,
2      5H  TC2)
2   FORMAT(/20X,25H REACTIVITY DISTURBANCE =,E10.3/)
111  FORMAT ( 20X, 31H PERCENT CHANGE IN SUBCOOLING =, E10.3/)
123  FORMAT( E10.3 )
124  FORMAT(20X,6H TWI =,E10.3/21X,5H QS =,E10.3)
      IF ( ISTRT - 1 ) 15 , 14 , 15
C
14   FAC1 = 0.66257628
      FAC2 = 0.60589151
C
      QS=42.9
      TWI=510.
      READ 123,CNTRD,QSD
      QTY = QSD * QS / 100.
      QS= QS + QTY
      TWI = TWI - QTY
      DELTA = CNTRD
      HZERO = 5.7595449
      TC1=620.
      TC2=600.
      AN=2.2727273E+08
      SSP=61.182837
      AK=SSP/AN
C
      B1=21.86867
      B2=0.057686028
      B3=0.28899514
      B4=7.40530330
      B5=21.868670
      B6=0.058794642
      B7=0.29454906

```

77132

(51)

```

BB=7.02008160
CONST=0.0216/0.4456
HIGHT=12.5
TSAT=544.6
TSW=(TWI+TSAT)/2.
PAI=4.*ATANF(1.)
FLOW=0.62489132
ALNTH=649.4
A2=.067592822
A4=.064076664
VOID1= 0.18635496
VOID = VOID1

```

```

CALL STAR
PRINT 2,CNTRD
PRINT 124 , TWI , QS
PRINT 111, QSD
CALL STAR
PRINT 1
CALL STAR
ISTRT = ISTRT + 1

```

```

1 YDASH(1)=-6.45*Y(1)+0.0124*Y(2)+0.0305*Y(3)+0.111*Y(4)+0.301
  *Y(5)+1.1*Y(6)+3.3*Y(7)+1000.*DELTA*(AN+Y(1))

```

```

YDASH(2)=0.21*Y(1) - 0.0124*Y(2)

```

```

YDASH(3)=1.41*Y(1) - 0.0305*Y(3)

```

```

YDASH(4)=1.27*Y(1) - 0.111*Y(4)

```

```

YDASH(5)=2.55*Y(1) - 0.301*Y(5)

```

```

YDASH(6)=0.74*Y(1) - 1.1*Y(6)

```

```

YDASH(7)=0.27*Y(1) - 3.3*Y(7)

```

```

POWER=AK*Y(1)
QMAX=(POWER/HIGHT)*(PAI/2.)
P1=FAC1*QMAX
P2=FAC2*QMAX

```

```

YDASH(8)=B1*P1 - B2*(Y(8)-Y(9))

```

```

YDASH(9)=B3*(Y(8)-Y(9))-B4*Y(9)

```

```

YDASH(10)= B5*P2 - B6*(Y(10)-Y(11))

```

```

YDASH(11) = B7*(Y(10)-Y(11)) - B8*(Y(11) - (QTY/2.))

```

TF AVG = ((HIGHT - HZERO) * Y(8) + HZERO * Y(10)) / HIGHT

TC1 = 620. + Y(9)

TC2 = 600. + Y(11)

VOIDD = VOID - VOID1

DELTA=(-9.E-04)*TF AVG - 0.1*VOIDD + CNTRD

RETURN

END

SIBFTC SUB4 NODECK,NOPRNT

SUBROUTINE CHANGE

DIMENSION X(20),V(20),AREA(20)

DIMENSION SPACE(215)

COMMON N

COMMON SPACE , ISTRT

COMMON ALNTH , HIGHT,HZERO,FLOW,PAI,QS,CONST,TSAT,TSW,TC1,TC2,A2,
1 A4,FAC1,FAC2,VOID

COSF(X)=COS(X)

PAV1 = A2*(TC1 - TSAT)*(HIGHT-HZERO)

PAV2 = A4*(TC2 - TSW)*HZERO

SUM = PAV1 + PAV2

QT= SUM/FLOW

A = ARCOS(1. - 2.*(QS/QT))

HZERO = HIGHT * A / PAI

CALCULATION OF NEW VALUES OF FAC1 AND FAC2

FAC1 = (1. + COSF(A)) / (PAI - A)

FAC2 = (1. - COSF(A)) / A

HINCT = (HIGHT - HZERO) / 20.

CALCULATION OF THE NEW VOID FRACTION

QMAX1 = (QT/HIGHT) * (PAI/2.)

START = COSF(A)

DO 10 J = 1 , 20

AJ = J

B = PAI * (HZERO + AJ * HINCT) / HIGHT

FINAL = COSF(B)

HEAT = (QMAX1*HIGHT / PAI) * (START - FINAL)

X(J) = HEAT / ALNTH


```

      AX = X(J)
      C = ( ( 1. - AX ) / AX ) * CONST * 2.
10    V(J) = 1. / ( 1. + C )
      AREA(1)=V(1)*HINCT/2.
      DO 30 J=2,20
30    AREA(J)=(V(J-1)+V(J))*HINCT/2.
      SUM1=0.
      DO 40 J=1,20
40    SUM1=SUM1 + AREA(J)
      VOID = SUM1 / HIGHT
C
C
      RETURN
      END
$IBFTC SUB5      NODECK,NOPRNT
      SUBROUTINE STAR
      PRINT10
      PRINT11
      PRINT10
10    FORMAT(1X)
11    FORMAT(1X,116H *****
1 *****
      RETURN
      END
$ENTRY

```

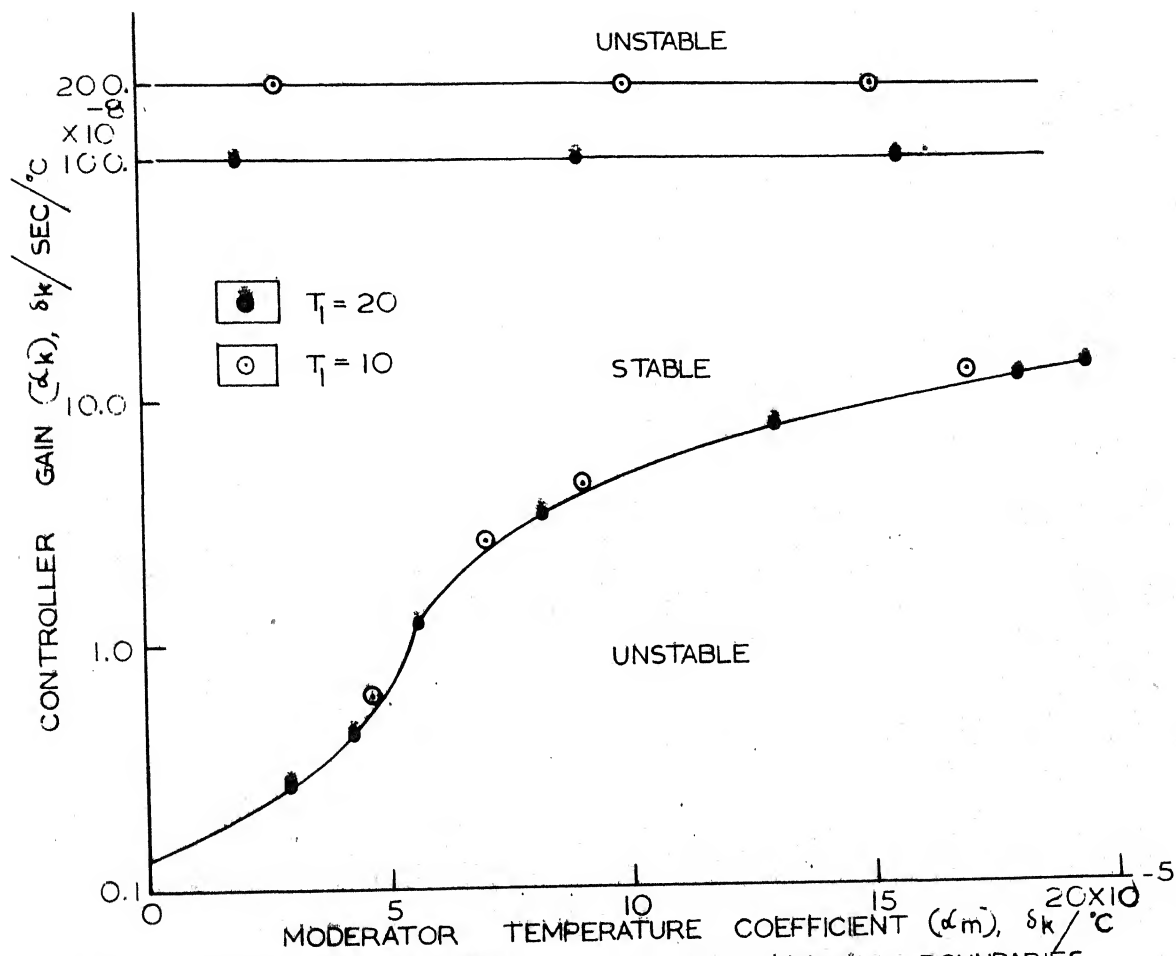


FIG. 1: EFFECT OF VARIATION OF T_1 ON STABILITY BOUNDARIES

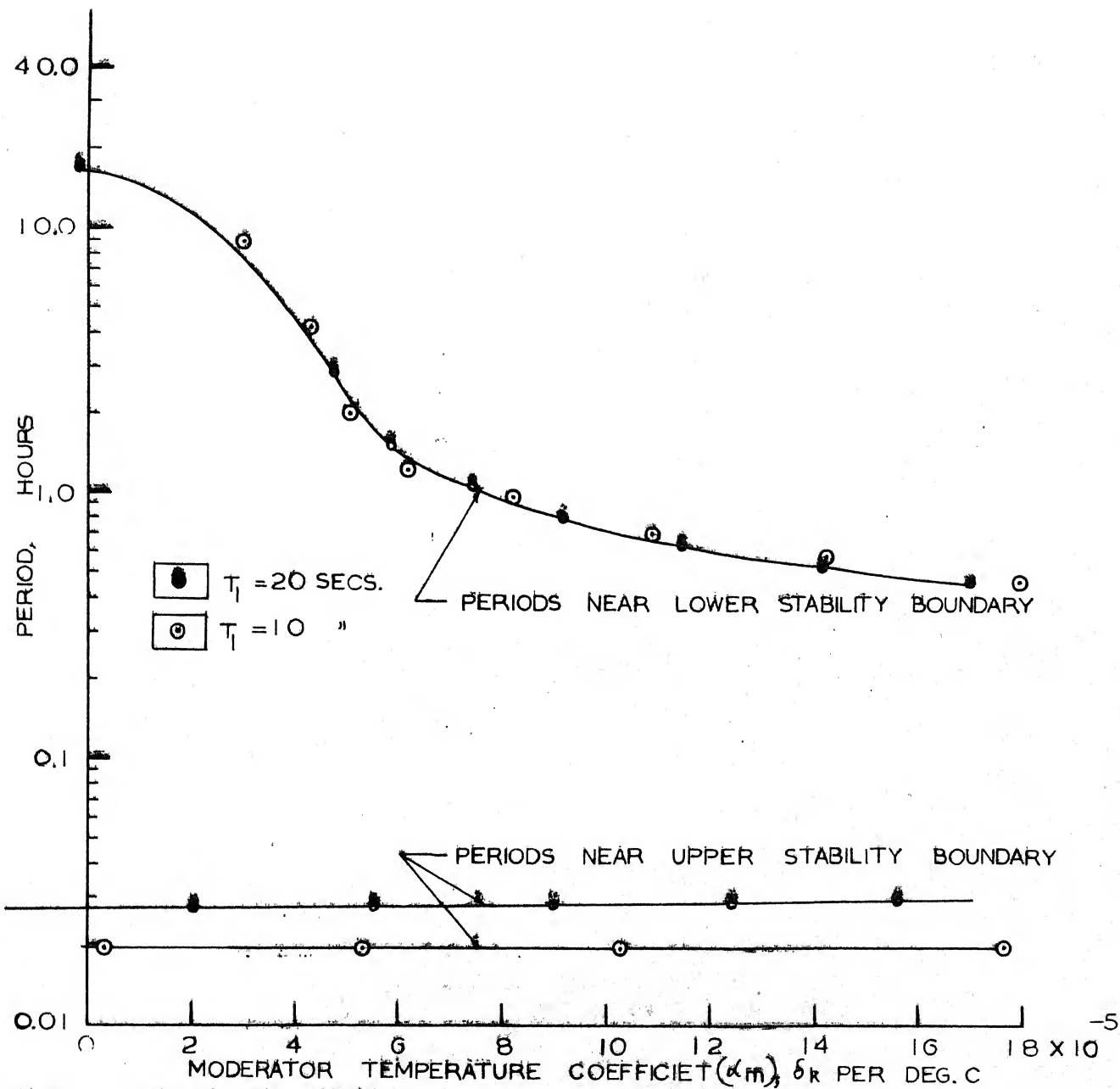


FIG. 2 EFFECT OF VARIATION OF T_1 ON PERIODS OF OSCILLATIONS.

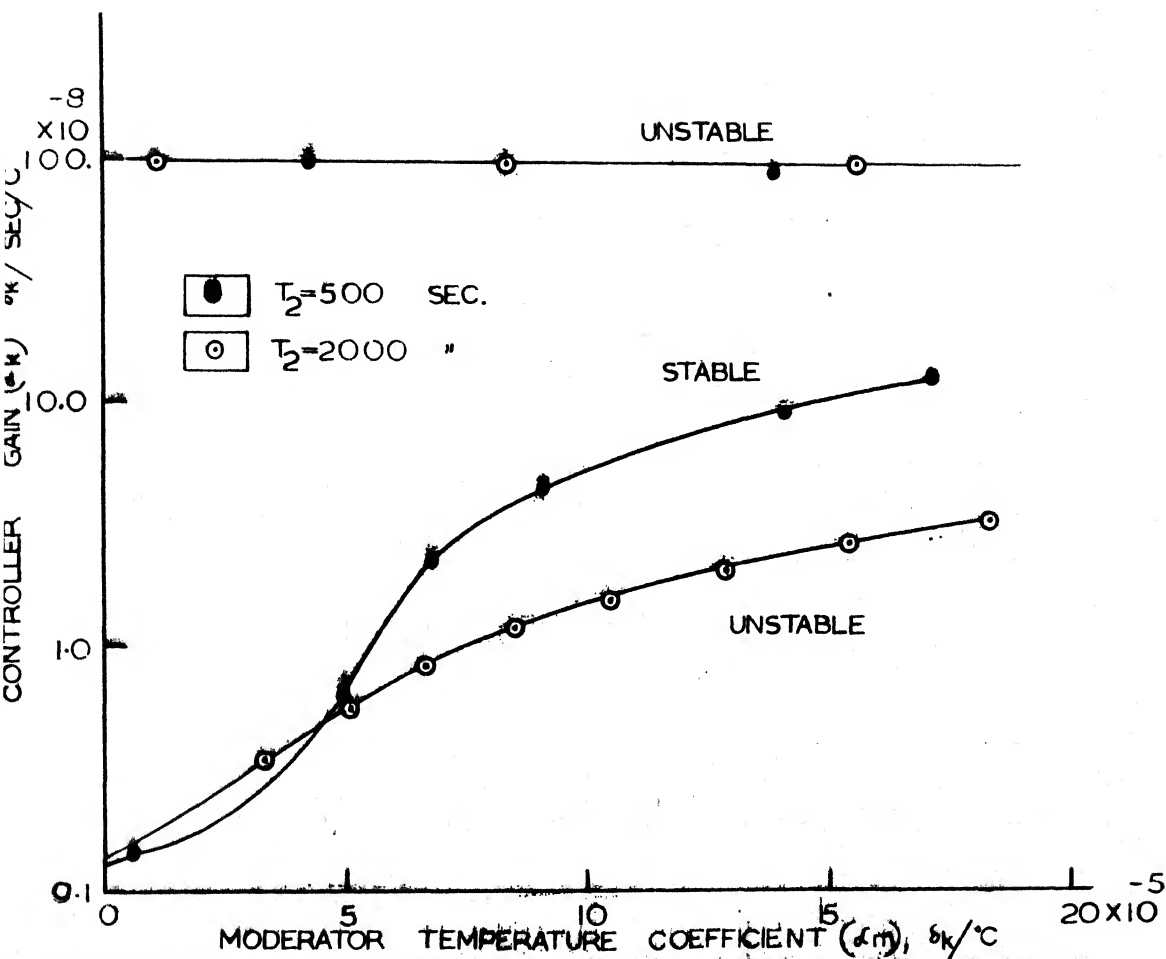


FIG.3 EFFECT OF VARIATION OF T_2 ON STABILITY BOUNDARIES.

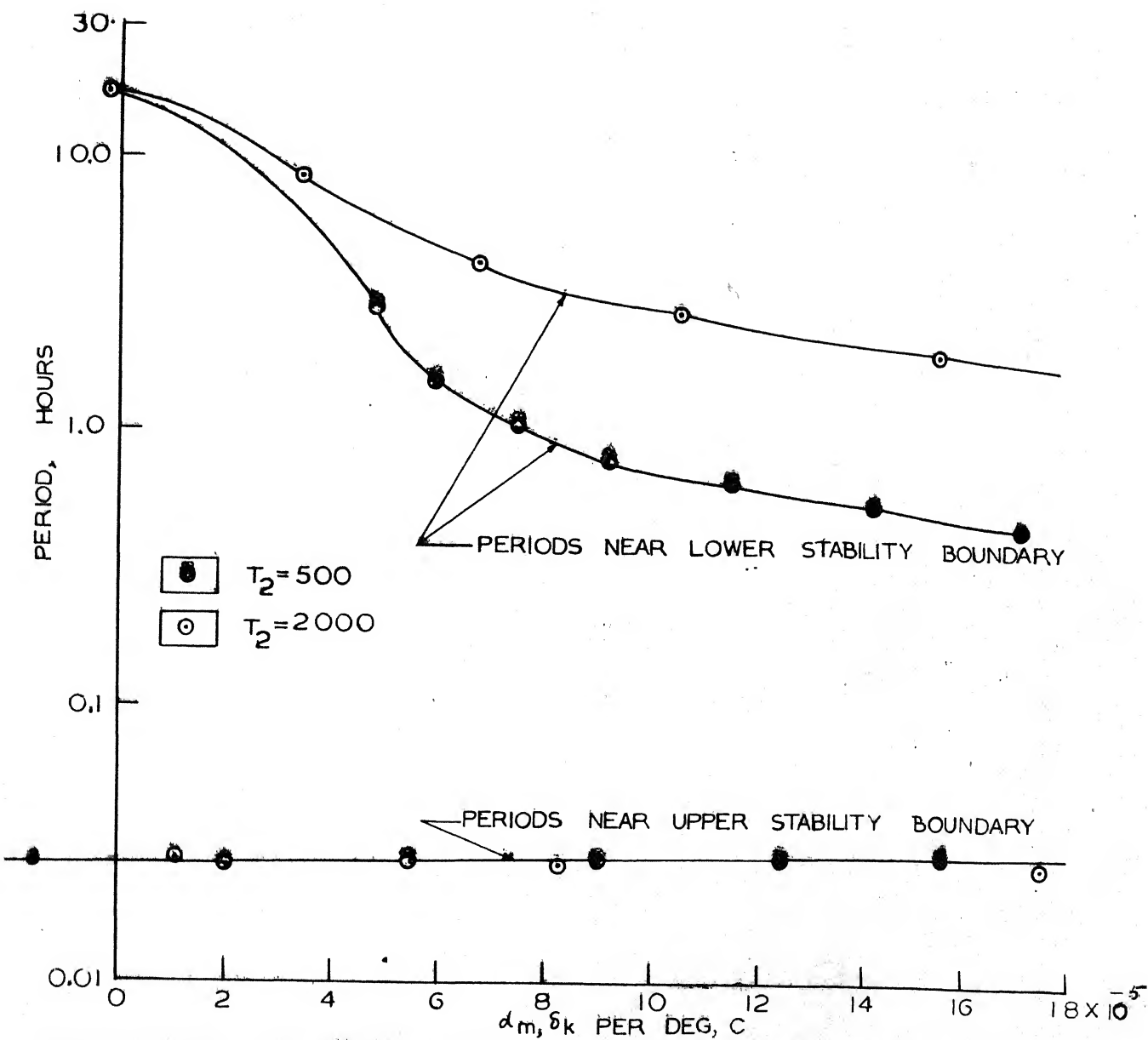


FIG.4: EFFECT OF VARIATION OF T_2 ON PERIODS OF OSCILLATIONS

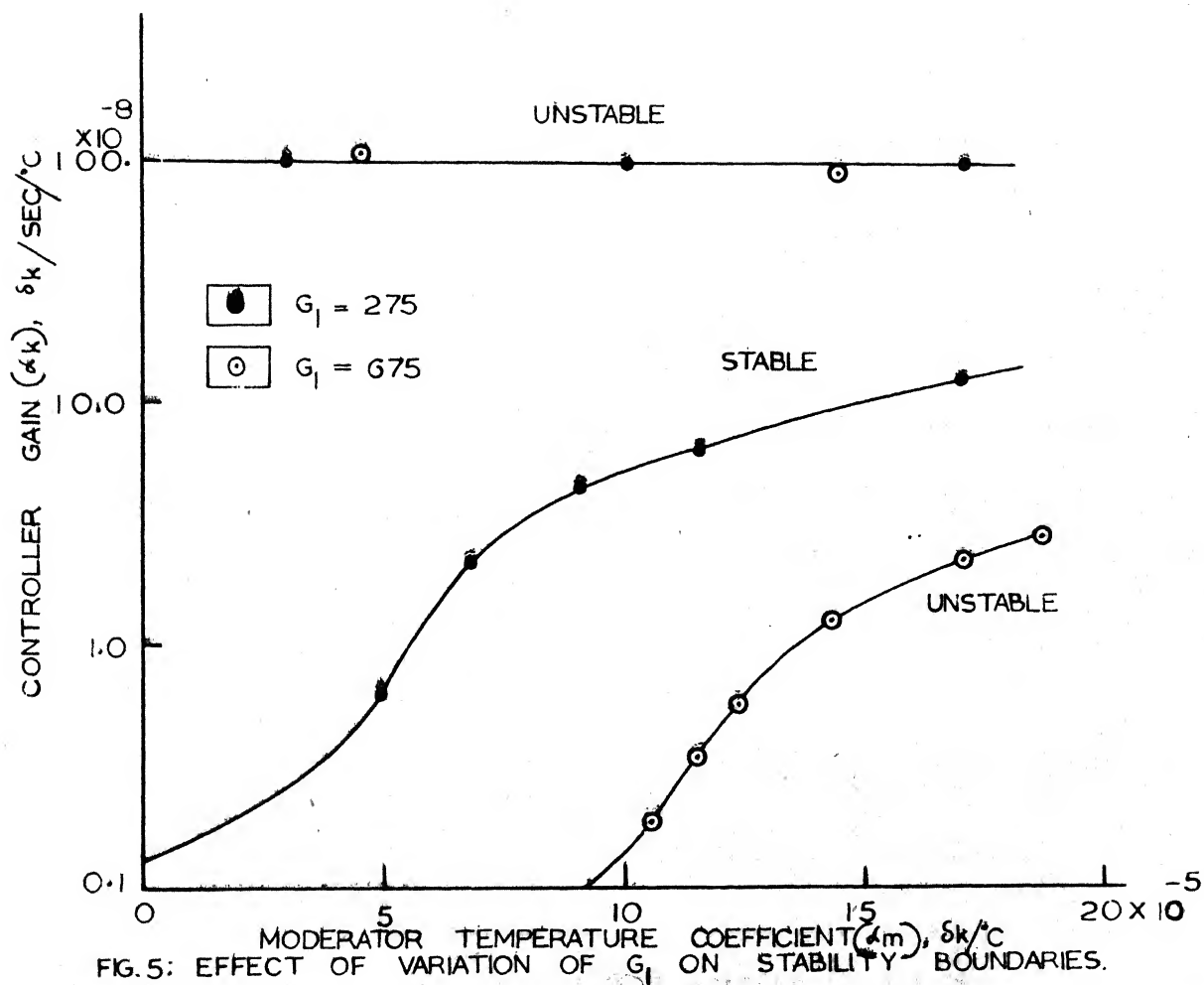


FIG. 5: EFFECT OF VARIATION OF G_1 ON STABILITY BOUNDARIES.

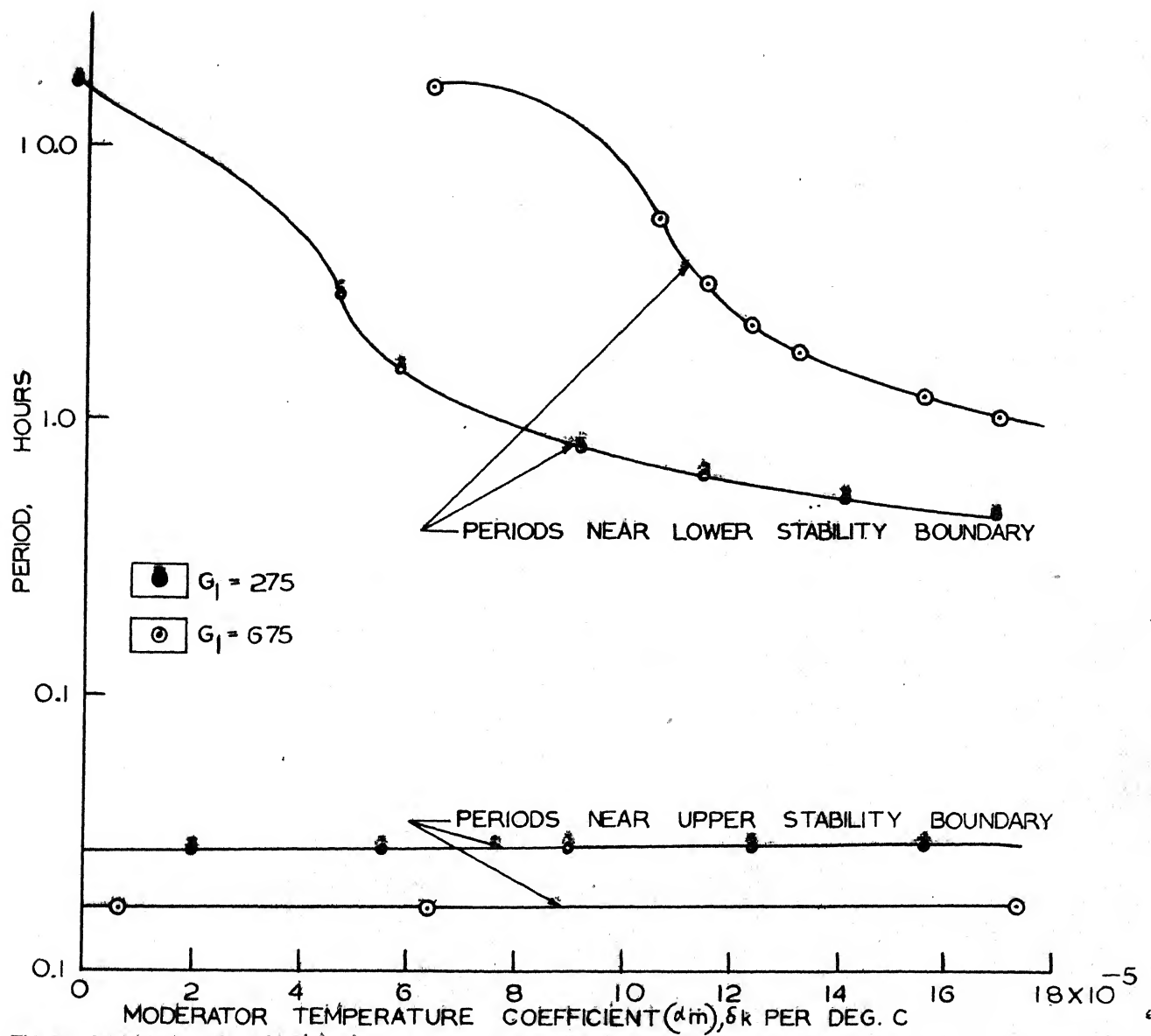


FIG.6 EFFECT OF VARIATION OF G_1 ON PERIODS OF OSCILLATIONS

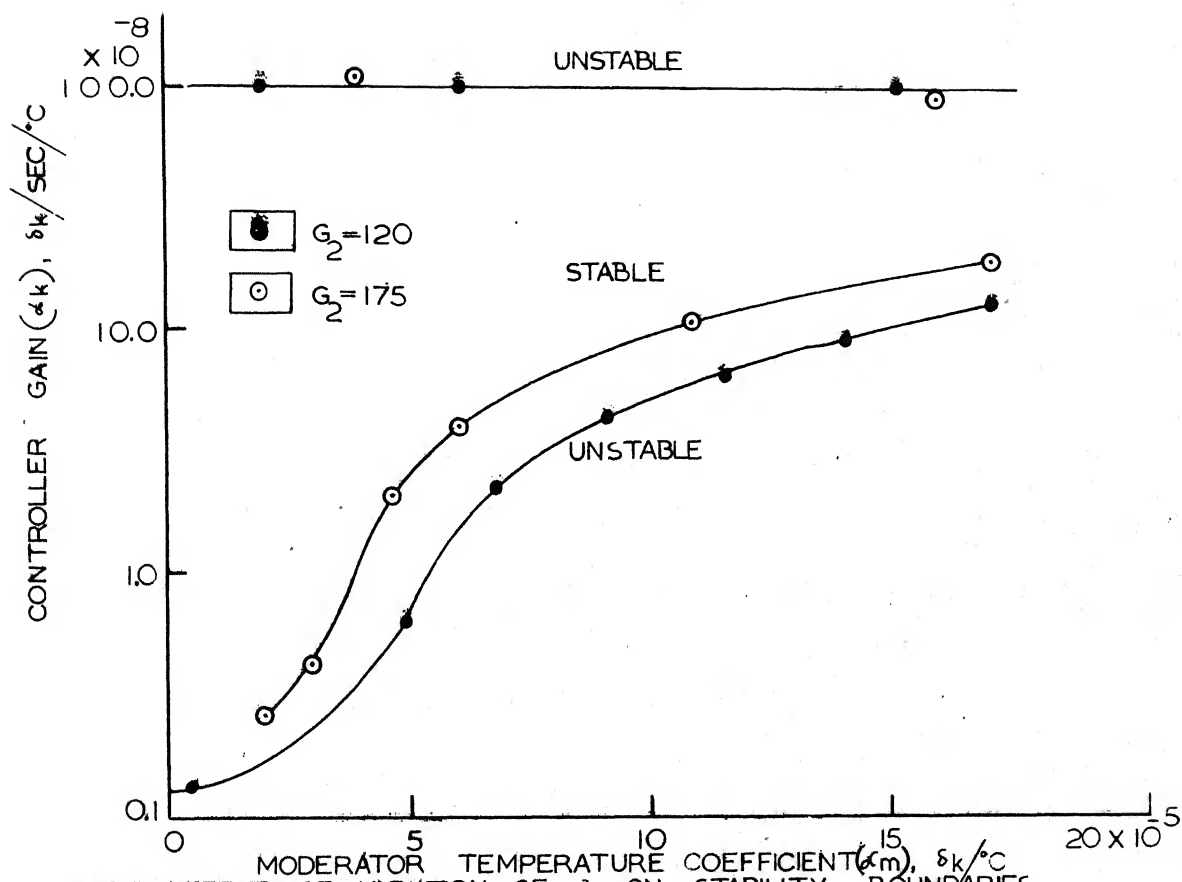


FIG. 7: EFFECT OF VARIATION OF G_2 ON STABILITY BOUNDARIES.

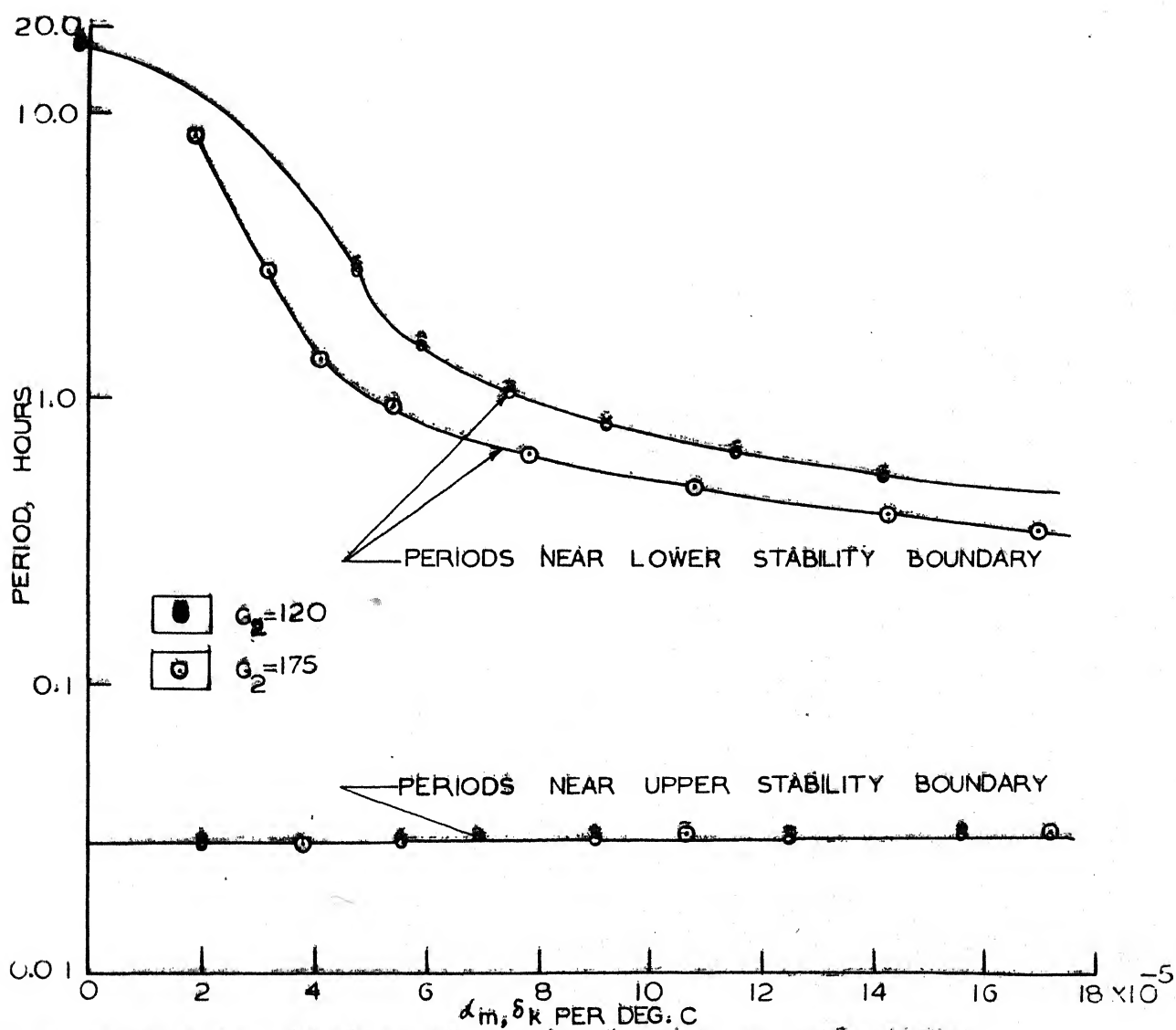


FIG. 8: EFFECT OF VARIATION OF G_2 ON PERIODS OF OSCILLATIONS

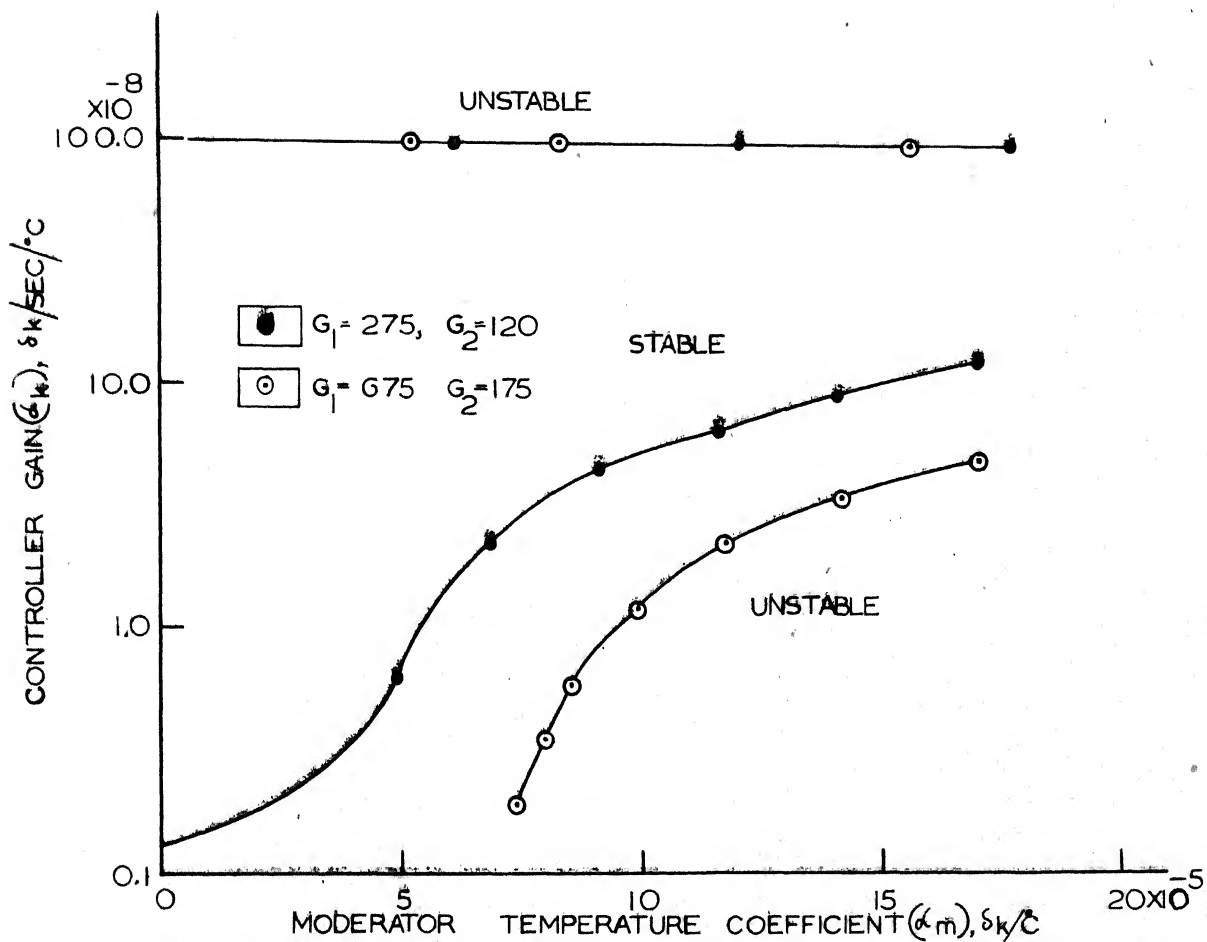


FIG.9: EFFECT OF SIMULTANEOUS VARIATION OF G_1 AND G_2 ON STABILITY BOUNDARIES.

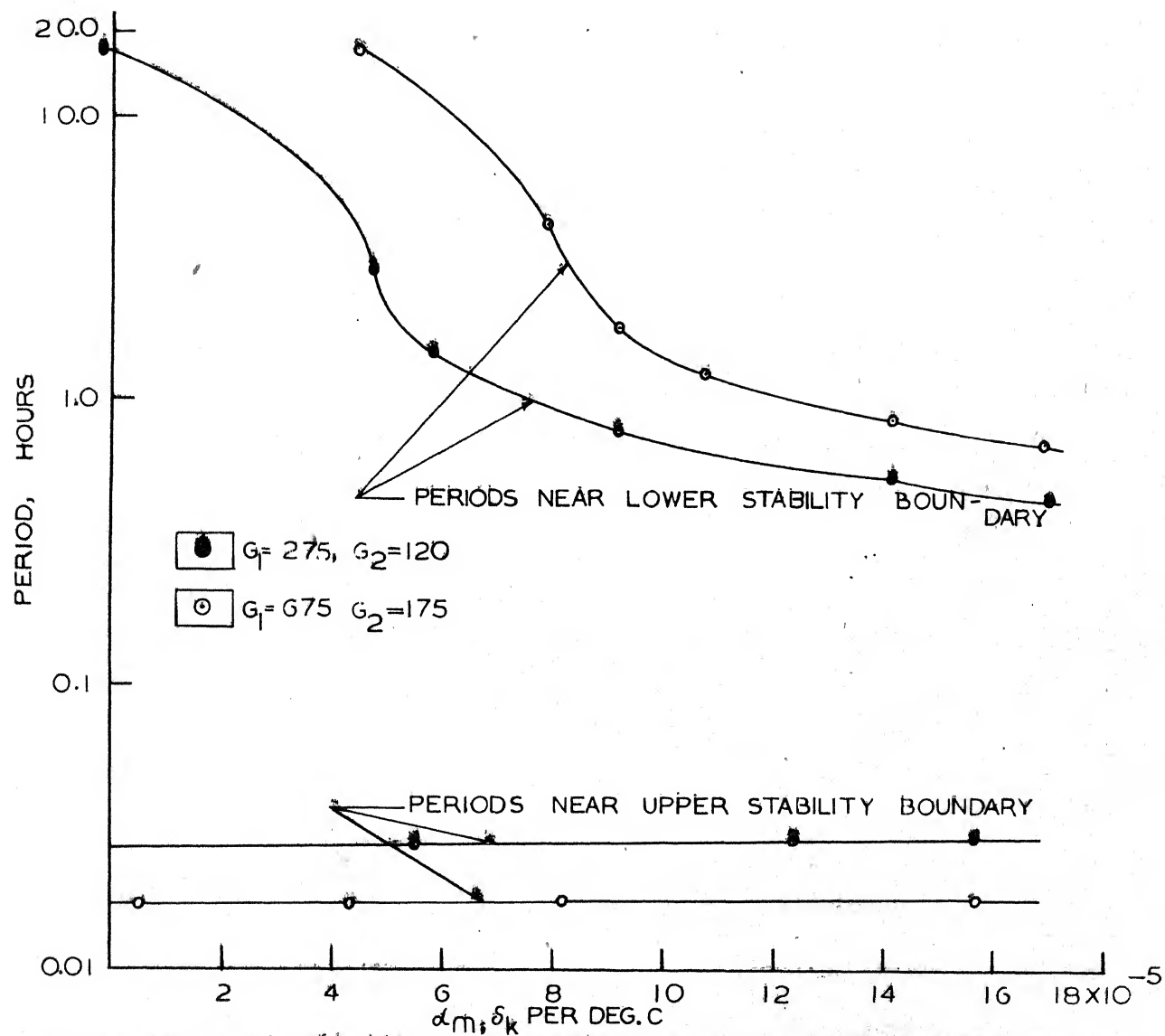


FIG.10 EFFECT OF SIMULTANEOUS VARIATION OF G_1 AND G_2 ON PERIODS OF OSCILLATIONS

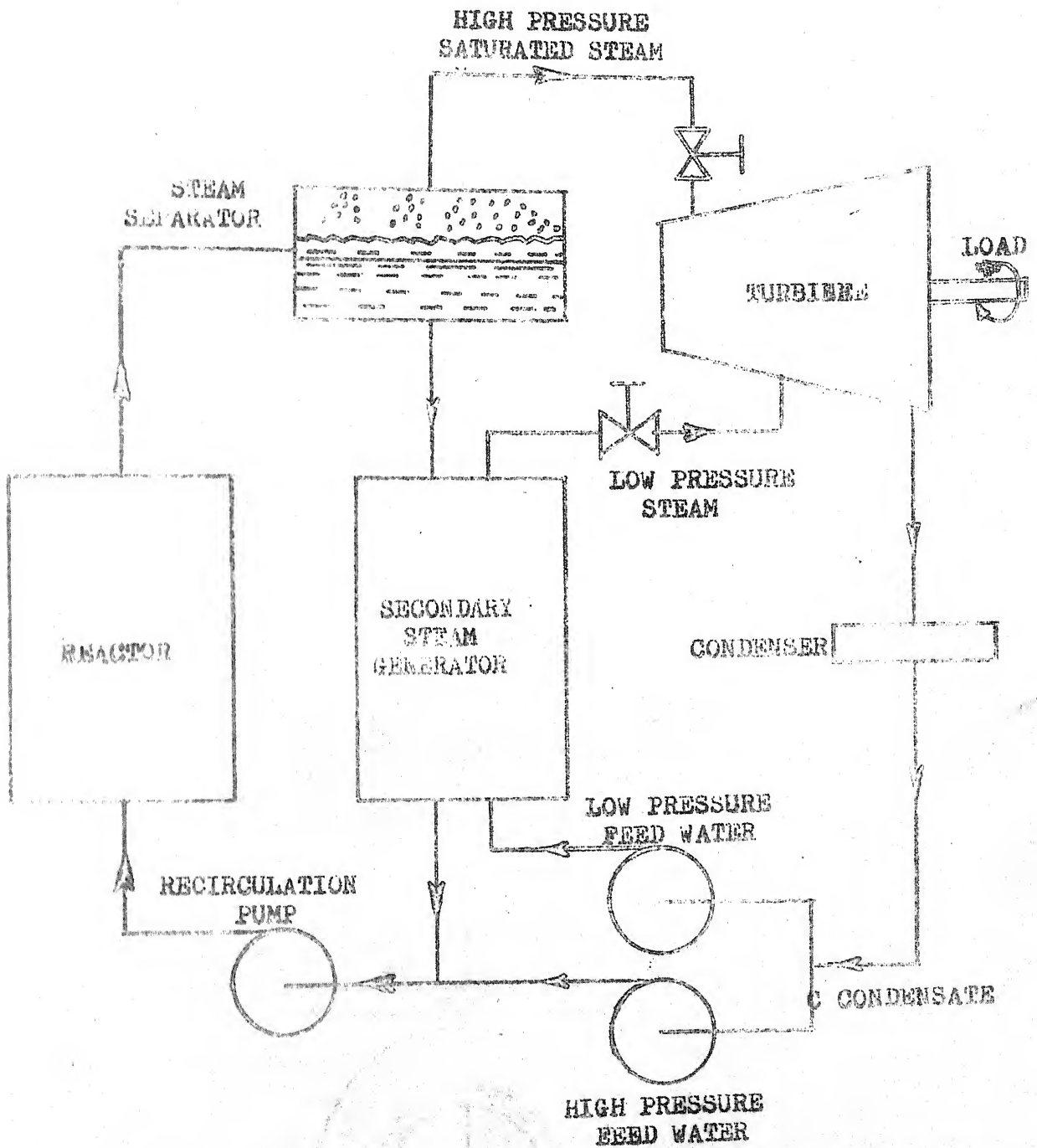


Fig. 11 Basic Elements of dual-cycle boiling-reactor power plant

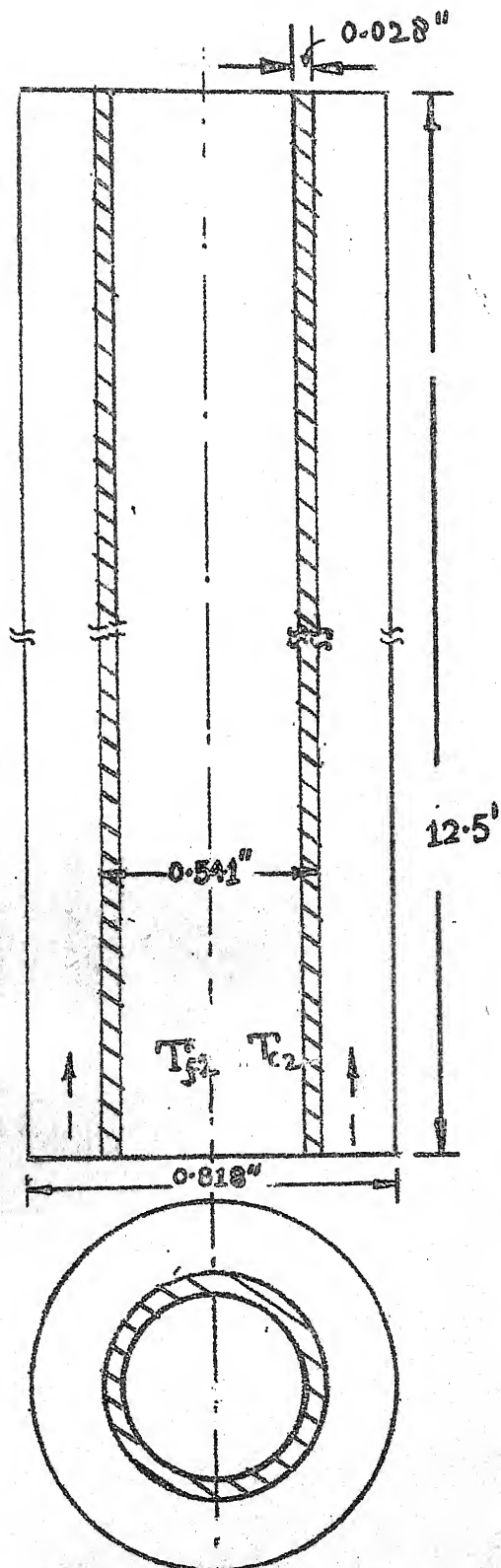


Fig.12. Dimensions of an average channel on the basis of a Unit Cell.

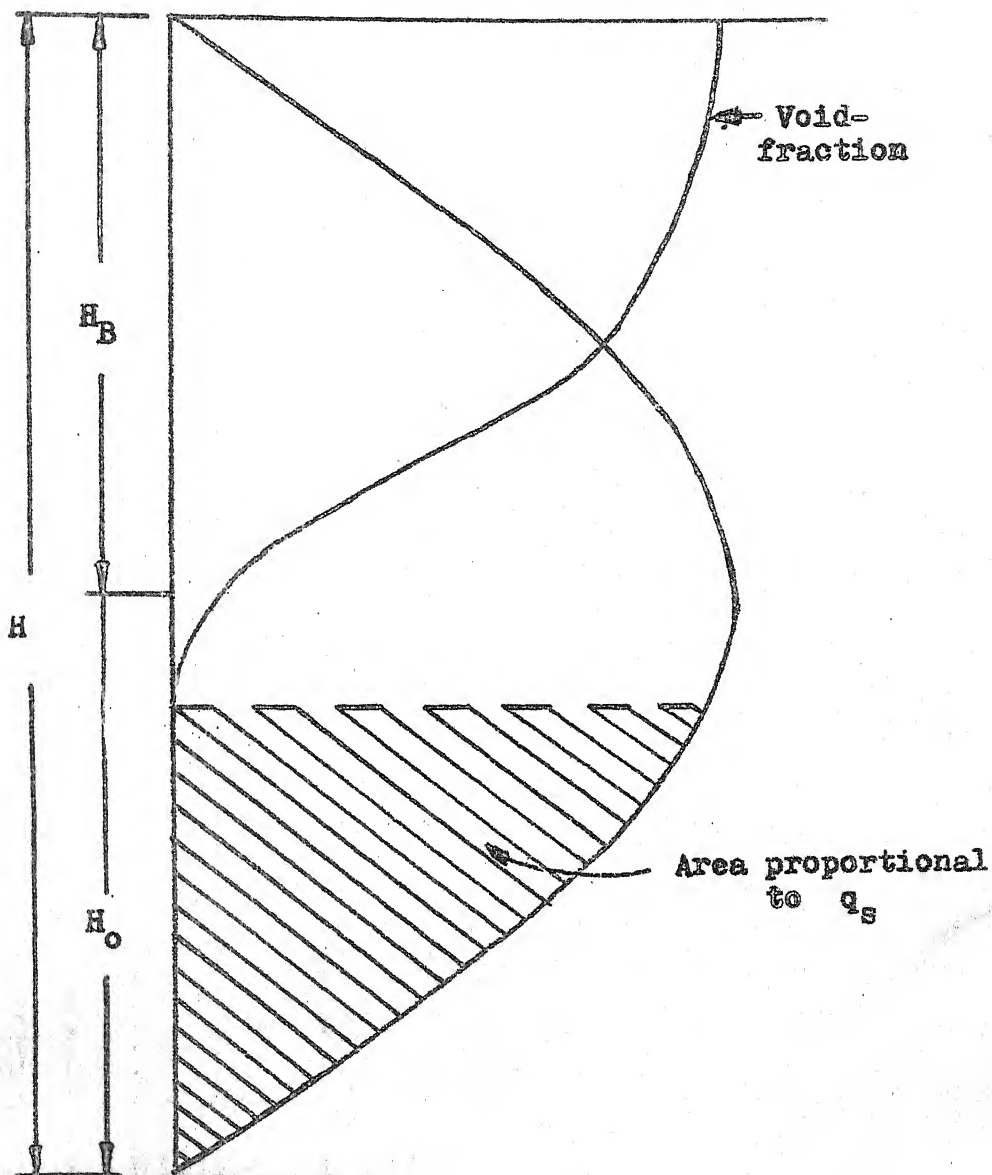


Fig. 13. Void fraction and non-boiling length with sinusoidal heat addition in a boiling channel.

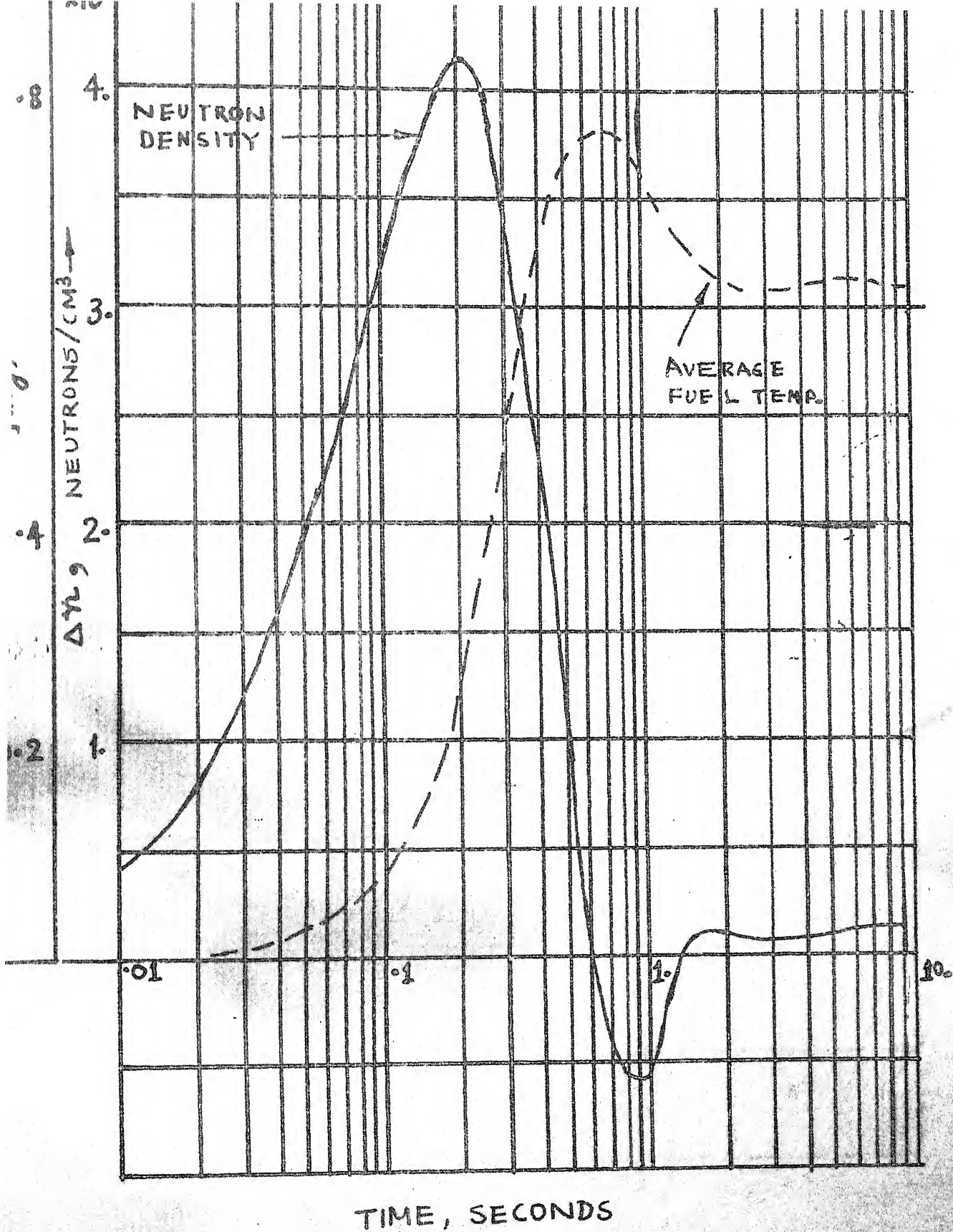


FIG. 14.

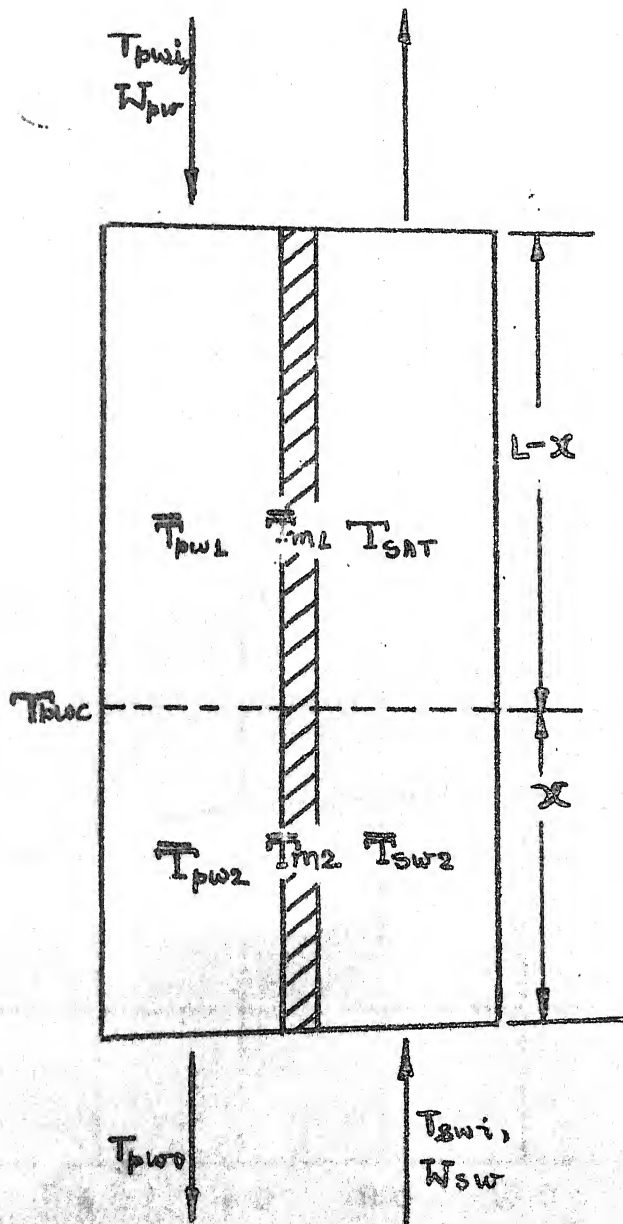
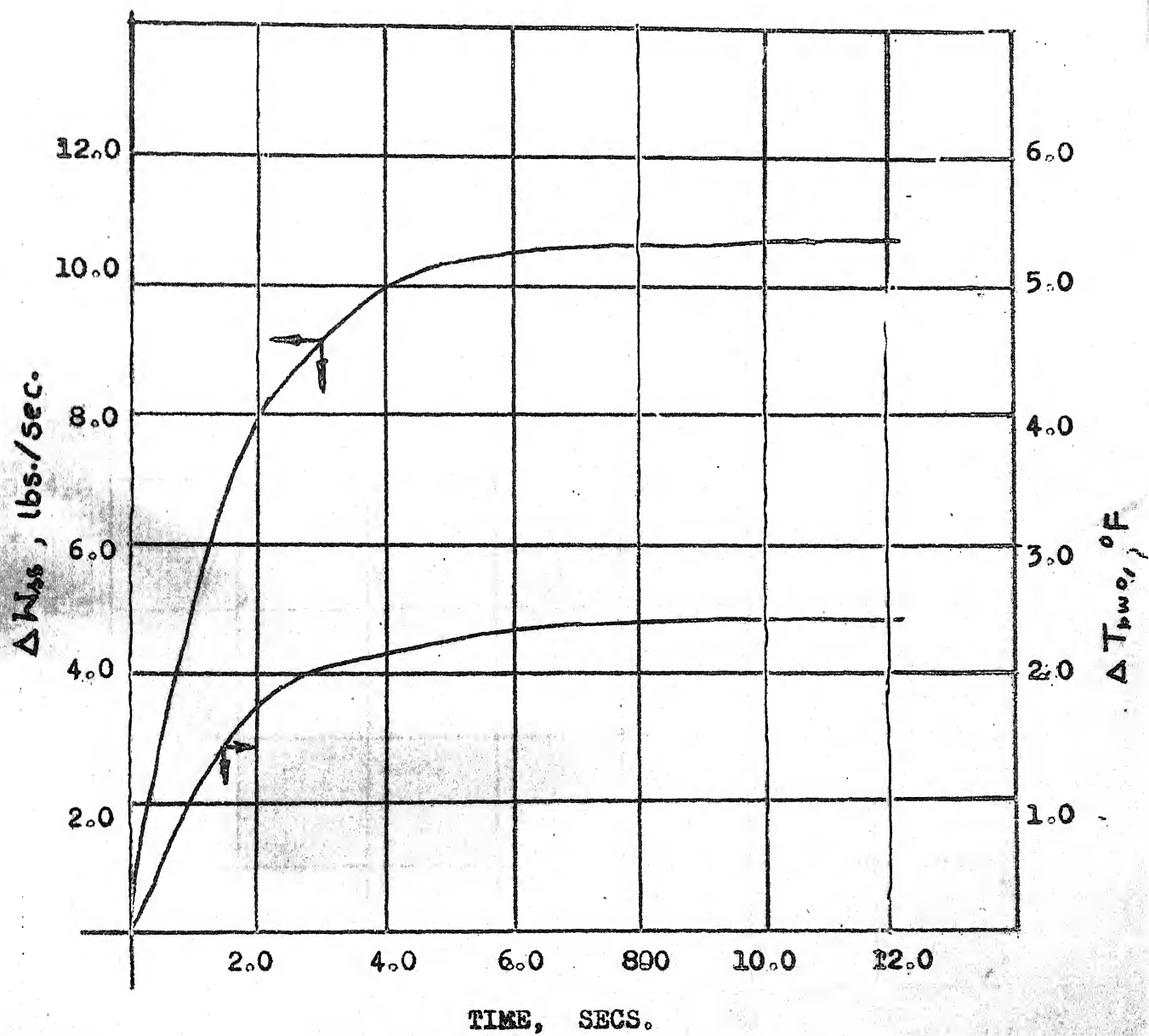
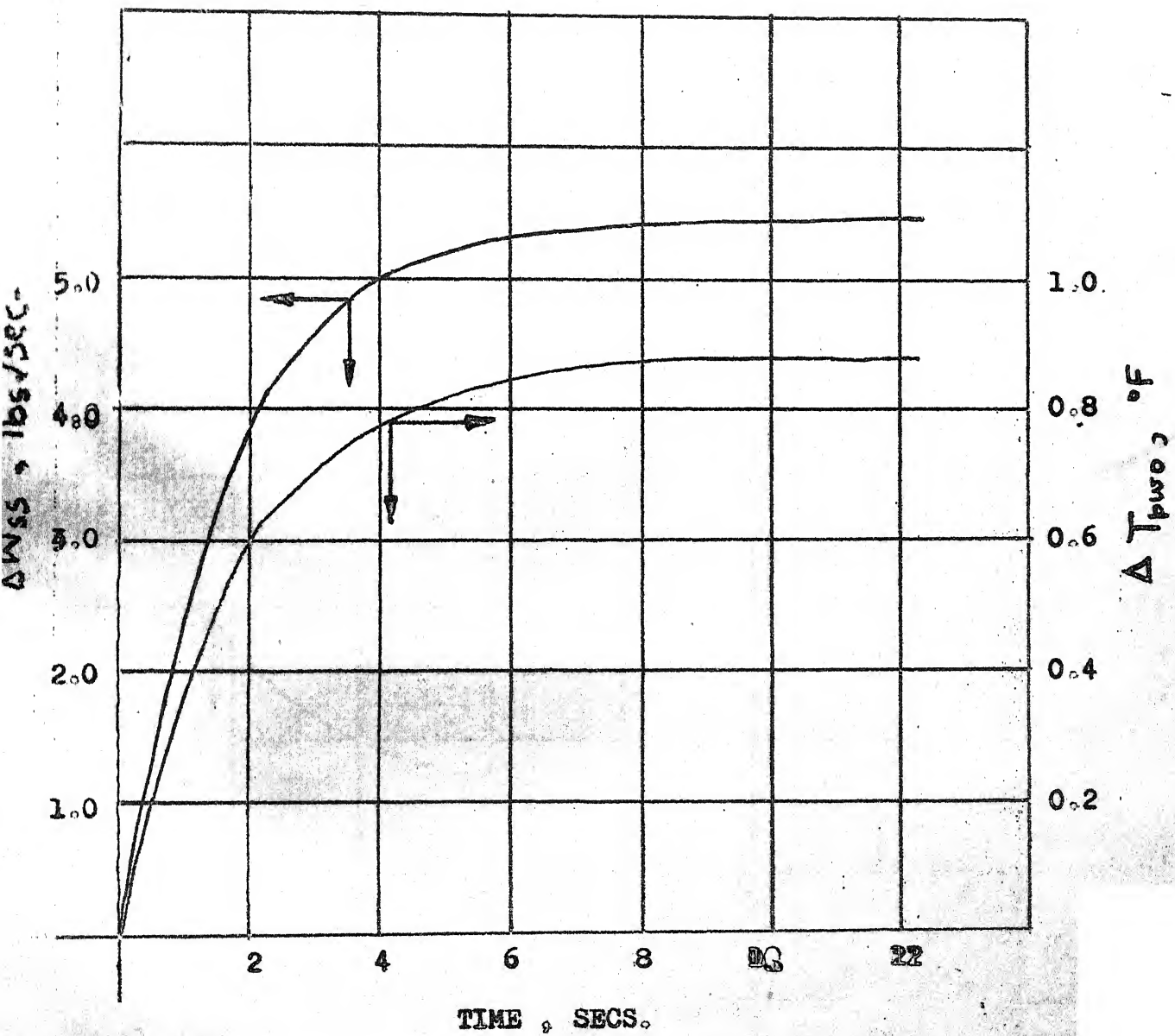


Fig.16. Secondary Steam Generator Model



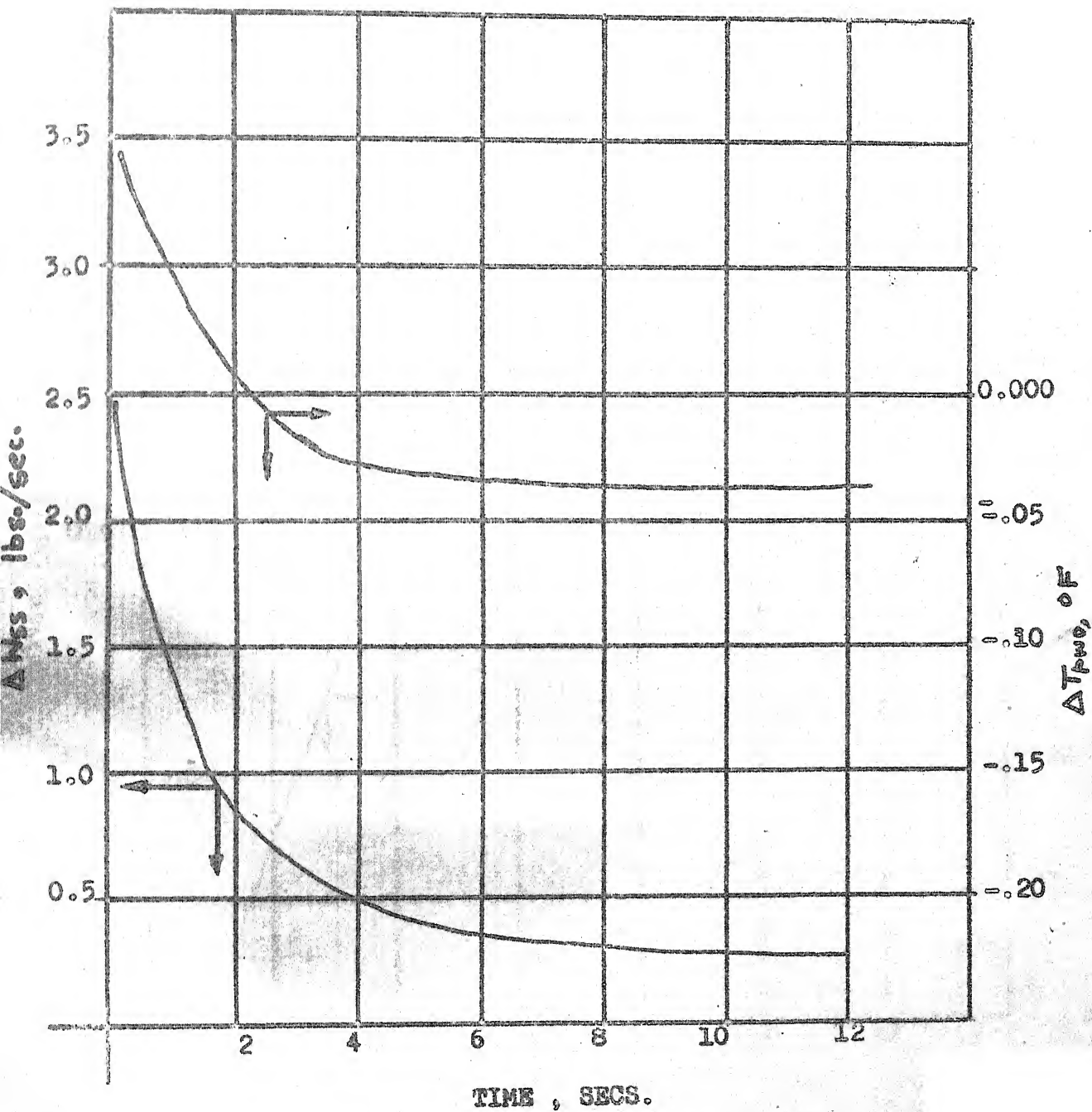
STEP CHANGE IN T_{pwi} AT TIME $t = 0$.

FIG. 17



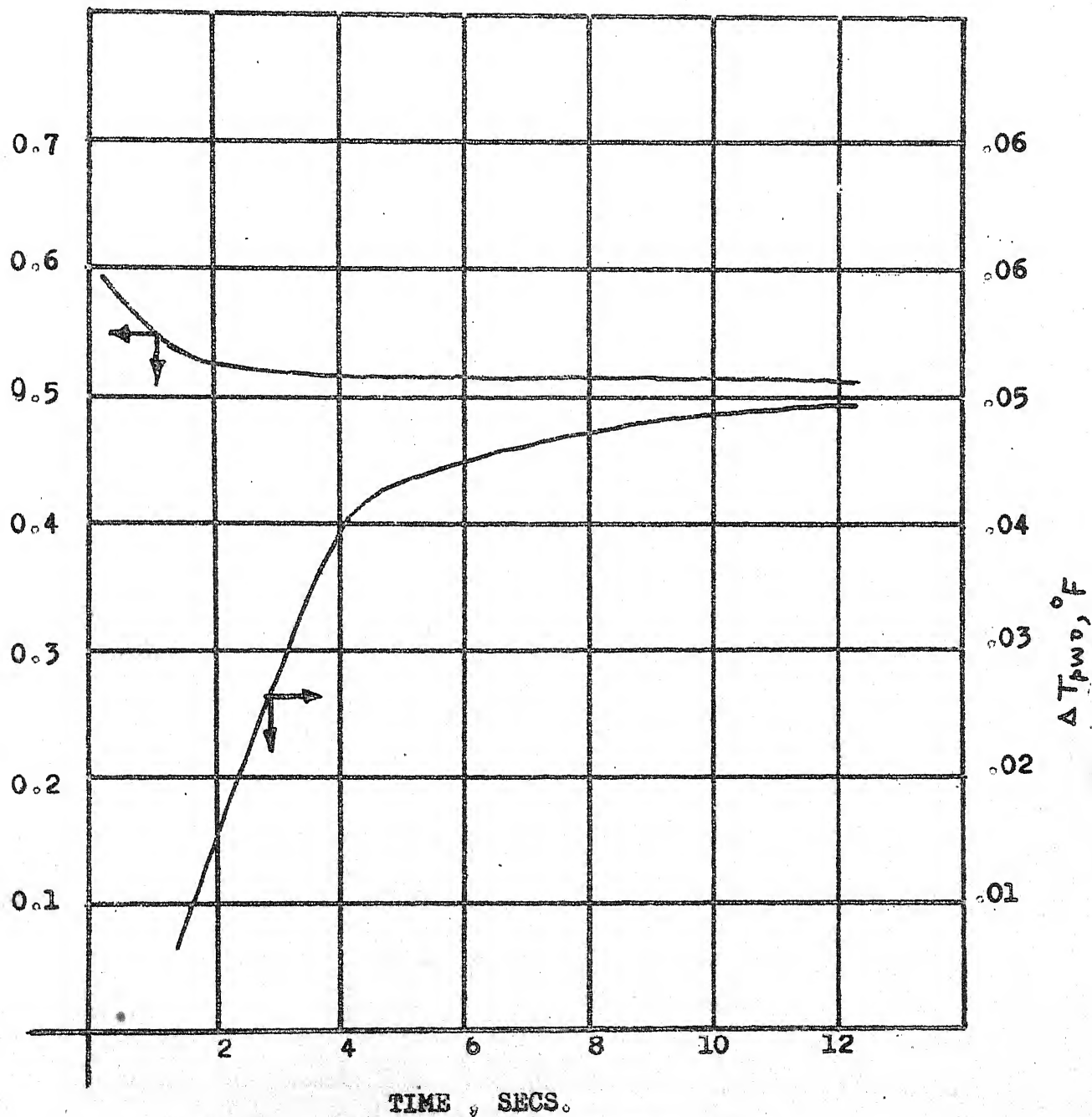
STEP CHANGE IN w_{pw} AT TIME $t = 0..$

Fig. 18



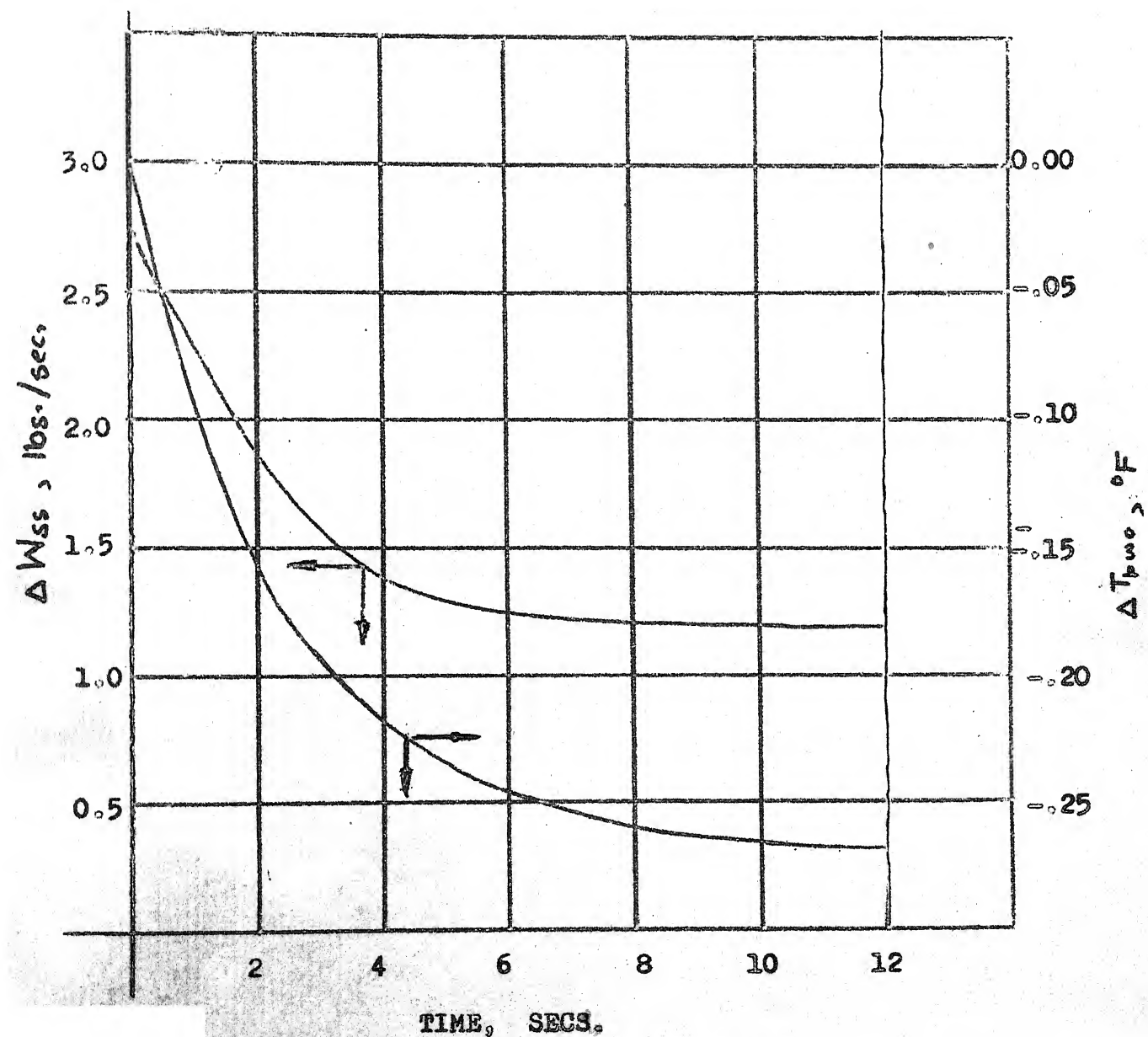
STEP CHANGE IN T_{swi} AT TIME $t = 0$

Fig. 19



STEP CHANGE IN w_{sw} AT TIME $t = 0$.

Fig. 20.



STEP CHANGE IN P_{sw} AT TIME $t = 0$

FIG. 21